

THE PENNSYLVANIA  
STATE UNIVERSITY

UNPUBLISHED PRELIMINARY DATA

NO 3 18 866

Code 1

# IONOSPHERIC RESEARCH

Scientific Report No. 188(E)

## PHASE AND ATTENUATION CHARACTERISTICS OF A VOLTAGE CONTROLLED ATTENUATOR

by

R. W. Vogt

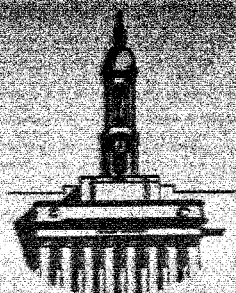
July 1, 1963

OTS PRICE

XEROX

MICROFILM

IONOSPHERE RESEARCH LABORATORY



University Park, Pennsylvania

NASA Grant No. NsG - 134-61

Ionospheric Research

NASA Grant No. NsG - 134-61

SCIENTIFIC REPORT

on

"Phase and Attenuation Characteristics of a  
Voltage Controlled Attenuator"

by


R. W. Vogt

July 1, 1963

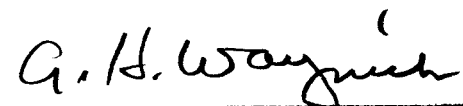
Scientific Report No. 188(E)

IONOSPHERE RESEARCH LABORATORY

Submitted by:

  
J. S. Nisbet, Assistant Professor of Electrical  
Engineering, Project Supervisor

Approved by:

  
A. H. Waynick, Professor of Electrical  
Engineering, Director of Ionosphere Research  
Laboratory

THE PENNSYLVANIA STATE UNIVERSITY

College of Engineering

Department of Electrical Engineering

CR-50,693

# TABLE OF CONTENTS

	Page
ABSTRACT . . . . .	i
1. INTRODUCTION . . . . .	1
1.1 Origin of the Problem . . . . .	1
1.2 General Statement of the Problem . . . . .	2
1.3 Review of Literature Pertinent to Transis-	
tor Automatic Gain Control Systems . . . . .	3
1.3.1 Forward and Reverse AGC . . . . .	3
1.3.2 Attenuators External to the	
Transistor . . . . .	4
1.4 Choice of Automatic Gain Control System . .	5
1.5 Specific Statement of the Problem . . . . .	6
2. PROCEDURE OF INVESTIGATION . . . . .	7
2.1 Design of the Attenuator . . . . .	7
2.1.1 Basic Principles of Operation . . .	7
2.1.2 Derivation of the Attenuator	
Equations . . . . .	10
2.1.3 Noise . . . . .	15
2.1.4 Sensitivity . . . . .	18
2.1.4.1 Rate of Change of Network	
Gain with Control Voltage .	18
2.1.4.2 Rate of Change of Logarith-	
mic Gain with Control Voltage	19
2.1.4.3 Second Derivative of	
Logarithmic Gain with Respect	
to Control Voltage . . . . .	20

2.1.4.4	Rate of Change of Phase with Control Voltage . . . . .	21
2.1.5	Relationship of Insertion Loss and Phase Shift to the Transformer Turns Ratio and Source and Load Impedances .	25
2.1.5.1	Insertion Loss . . . . .	25
2.1.5.2	Overall Phase Shift . . . . .	25
2.1.5.3	Optimum Design . . . . .	29
2.1.6	Temperature Effects and Stability . .	32
2.1.6.1	Zener Diodes . . . . .	32
2.1.6.2	Capacity Diodes . . . . .	35
2.2	Experimental Procedure and Results . . . . .	37
2.2.1	Measurement of Attenuation as a Function of Control Voltage . . . . .	37
2.2.2	Overall Phase Shift Measurement . . .	43
2.2.3	Optimum System Performance Tests . . .	46
2.2.4	Temperature Measurements . . . . .	55
2.2.4.1	Capacity Diode . . . . .	55
2.2.4.2	Bridge Transformer . . . . .	55
2.2.4.3	Complete Attenuator System .	59
3.	SUMMARY AND CONCLUSIONS . . . . .	60
APPENDIX A	The Voltage Sensitive Capacity Diode . . .	63
APPENDIX B	Description of the 54MC/S Phase Comparator	70
BIBLIOGRAPHY	. . . . .	73
ACKNOWLEDGEMENTS	. . . . .	75

ABSTRACT

18866

An analysis of a small phase shift, voltage controlled attenuator, suitable for automatic gain control, is presented.

The factors which affect the relationship of the attenuation to the phase shift are found and criteria are developed for selecting circuit parameters to give minimum phase change for a given attenuation.

## 1. INTRODUCTION

### 1.1 Origin of the Problem

In a proposed rocket experiment by Nisbet et al., (1960), measurements are made of the relative phase shifts of radio waves propagated between two sections of a high altitude research rocket. It was shown that these phase shifts are directly related to the electron density along the propagation path between the two. Signals at each of the three frequencies at the main rocket section are amplified and compared in phase. The amplitude of these signals will vary due to the increasing path length, changing effective area of the antenna, and due to ionospheric detuning of the antennas. It is necessary to be able to make a measurement of the phase unperturbed by these effects. It is also necessary for the measurement of secondary parameters in this experiment to have information on the signal intensity as a function of time and a signal strength output is required.

The experiment is to be conducted using a research rocket in which payload weight is at a premium. These requirements on payload and space are such that transistorized circuitry is mandatory.

In order to achieve the desired accuracy, the maximum phase shift for each channel is required to

be less than  $\pm 15$  degrees when compared to the reference intermediate frequency. A further requirement is a maximum gain of 72 db., with an automatic gain control (AGC) providing a constant output within 3 db., over a dynamic range of 60 db.

It is therefore desirable to have a transistorized receiver with a large dynamic range of AGC and a very small internal phase shift.

It should be noted that though the requirement generating this problem is rather specialized, many other applications such as in direction finding equipment require receivers having small phase shifts over wide ranges of input signal strength.

## 1.2 GENERAL STATEMENT OF THE PROBLEM

In receivers used for phase measurements it is necessary to minimize the internal phase distortion while providing an AGC system which automatically varies the total amplification and maintains the power output almost constant for large variations of input signal strengths.

When the AGC signal acts to alter the bias conditions in controlling transistor gain, the resultant effects are a shift in bandwidth and in center frequency due to changes in the input and output impedances. A summary of literature relating the methods which have been used is given in Section 1.3 .

The problem, then, is to find an AGC system capable of providing easily controlled attenuation and minimum phase shift. In addition, this device should be of minimum size, weight, temperature sensitivity and complexity.

### 1.3 REVIEW OF THE LITERATURE PERTINENT TO TRANSISTOR AUTOMATIC GAIN CONTROL SYSTEMS

#### 1.3.1 FORWARD AND REVERSE AGC

The most common method of gain control is that in which the bias conditions of the transistor are controlled. The gain may be varied by changing the emitter current or the collector voltage; each of these techniques results in a change in bandwidth and a shift in center frequency.

Blecher (1953) demonstrated that the gain of a transistor could be varied by changing the direct current in the emitter-base junction.

Chow and Stern (1955) investigated gain control by changing the collector voltage or emitter current and discussed the resulting effects upon the transistor parameters. This paper also showed that forward AGC (emitter current control) was accompanied by increasing input and output impedances which caused a decrease in bandwidth and a shift in center frequency. Reverse AGC (collector voltage control), however, showed the effects of decreasing input and output impedances resulting in an increase in bandwidth and a



shift in center frequency. It was concluded that in cases where it is desirable to keep the bandwidth constant it is necessary to place the frequency selective circuits in stages not adjoining controlled stages.

Seliga (1961) et al., have shown that the magnitudes of the phase shifts for forward and reverse AGC systems were nearly equal for equal changes in gain; the senses of the phase shift for these conditions are different however, suggesting a possible method of phase compensation. In Seliga's paper it was shown that for an 11 mc/s amplifier stage and a 30 db. change of attenuation, forward AGC produced a phase shift of 70 degrees, while reverse AGC produced a phase shift of - 60 deg.

### 1.3.2 ATTENUATORS EXTERNAL TO THE TRANSISTOR

Hurtig (1955) developed a circuit to limit changes in bandwidth by placing a diode in parallel (from the a.c. viewpoint) with the emitter diode of the transistor. This scheme divides the signal current between the diodes in accordance with the AGC signal in such a way that the conductance of the diode combination remains essentially constant.

At 9 mc/s this circuit produced a 40 kc/s change in bandwidth (B.W. = 1.4 mc/s) and a change in center frequency of 72 kc/s for 42 db. of attenuation.

Chow and Lazar (1959) used a system utilizing back-biased diodes in a bridge configuration. The method discussed in this paper is one which may be used to:

1. Control a signal which has a dynamic range exceeding the capabilities of the first amplifier
2. Reduce the net gain of the stage below unity
3. Control gain where very low control power is available.

While the attenuation characteristics of the AGC network appeared to be satisfactory, no mention of its frequency characteristics was made.

#### 1.4 CHOICE OF AUTOMATIC GAIN CONTROL SYSTEM

It can be seen from the literature summary that the techniques used in the past have produced phase shifts which are larger than the maximum phase change tolerable in the proposed rocket experiment.

The rather stringent phase shift requirements and the desire to keep the system simple precludes obtaining the gain variation by controlling the transistor parameters.

One system (Chow and Lazar) which had good attenuation characteristics (60 db. attenuation) also had the potential of a small phase change characteristic. In addition, it was simple in design, controlled with low power, and simplified the receiver design. Each receiver stage can be operated with fixed bias conditions, thus permitting the optimization of gain, noise figure, bandwidth, stability, and the number of components necessary.

#### 1.5 SPECIFIC STATEMENT OF THE PROBLEM

1. To analyze a voltage controlled attenuator bridge circuit, in which the attenuation is obtained by balancing a bridge consisting of two voltage sensitive capacity diodes (VSCD).
2. To determine the factors which affect the relationship of the attenuation to the phase shift and to develop criteria for selecting circuit parameters to give minimum phase change for a given attenuation.
3. To examine the stability of the circuit under environmental changes such as temperature.
4. To compare the phase characteristic of this method of AGC with those using forward and reverse AGC.

## 2. PROCEDURE OF INVESTIGATION

### 2.1 DESIGN OF THE ATTENUATOR

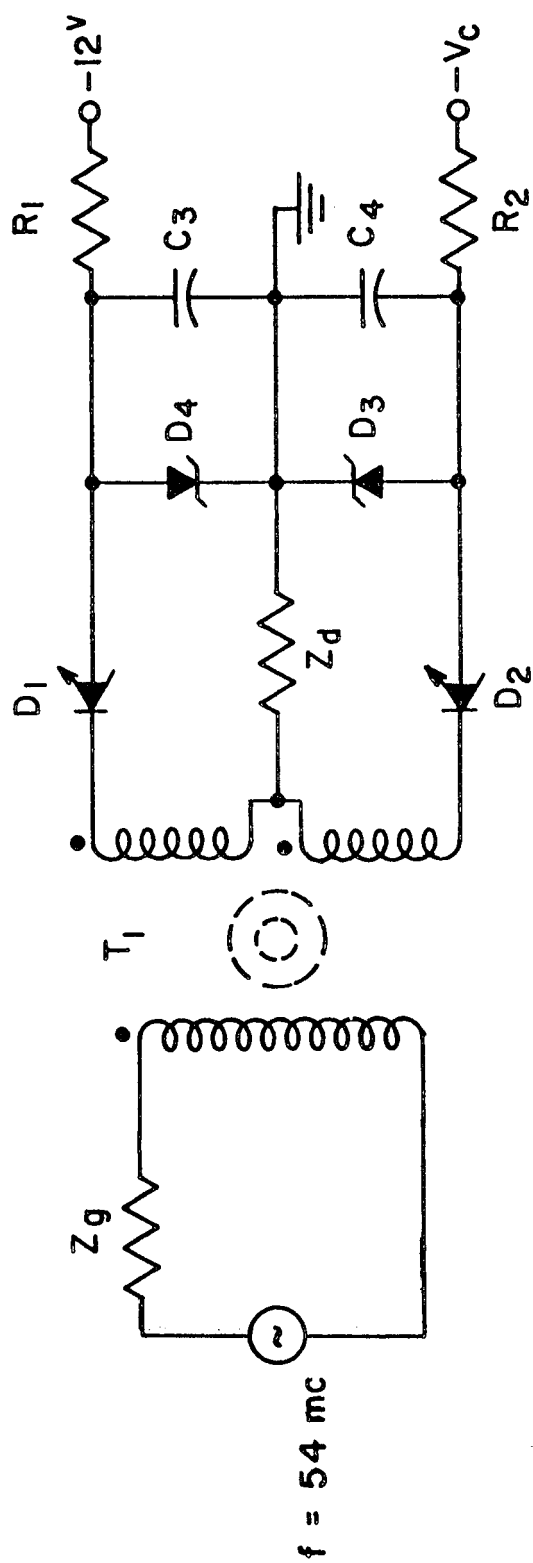
#### 2.1.1 BASIC PRINCIPLE OF OPERATION

The AGC mechanism selected consists of a bridge attenuator with a fixed gain receiver used as the detector. In one arm of the bridge a reverse-biased silicon diode is included in such a manner that its capacitance can be controlled by a d.c. voltage. By controlling the d.c. voltage, the bridge may be made to approach the balance condition introducing a large attenuation between the input and output terminals.

If the d.c. control voltage is derived from the receiver output, an automatic gain control characteristic may be obtained for the system.

A circuit which uses this principle is shown in Figure 1. The reverse-biased diodes (capacity diodes) and the zener diodes are known to have temperature coefficients which are, in general, small. To further reduce the temperature effects, similar diodes are used in each arm of the bridge which tends to self-compensate for temperature variations.

Zener diodes are used to prevent damage to the capacity diodes due to excessive reverse-bias.



# BRIDGE ATTENUATOR CIRCUIT

## FIGURE 1

$R_1, R_2 = 750 \Omega$   
 $C_3, C_4 = .001 \mu f$   
 $D_1, D_2 = V-100$   
 $D_3, D_4 = IN936A$

The zener diodes also ensure that equal bias voltages are presented to the capacity diodes under the condition of maximum control voltage.

A small trimmer capacitor can be placed in parallel with the fixed-bias diode to compensate for dissimilar voltage characteristics of practical zener and capacity diodes and to prevent the possibility of going beyond the balance point.

The bridge transformer with a bifilar wound secondary is used to take the place of passive elements in the arms of the usual bridge circuit configuration. The transformer used in this manner eliminates some power loss and provides an accurately balanced source impedance. An electrostatic shield is incorporated in the transformer to reduce the capacitive coupling between the primary and secondary windings.

### 2.1.2 DERIVATION OF THE ATTENUATOR EQUATIONS

A schematic diagram of the bridge attenuator network is shown in Figure 1 and its equivalent circuits in Figure 2.

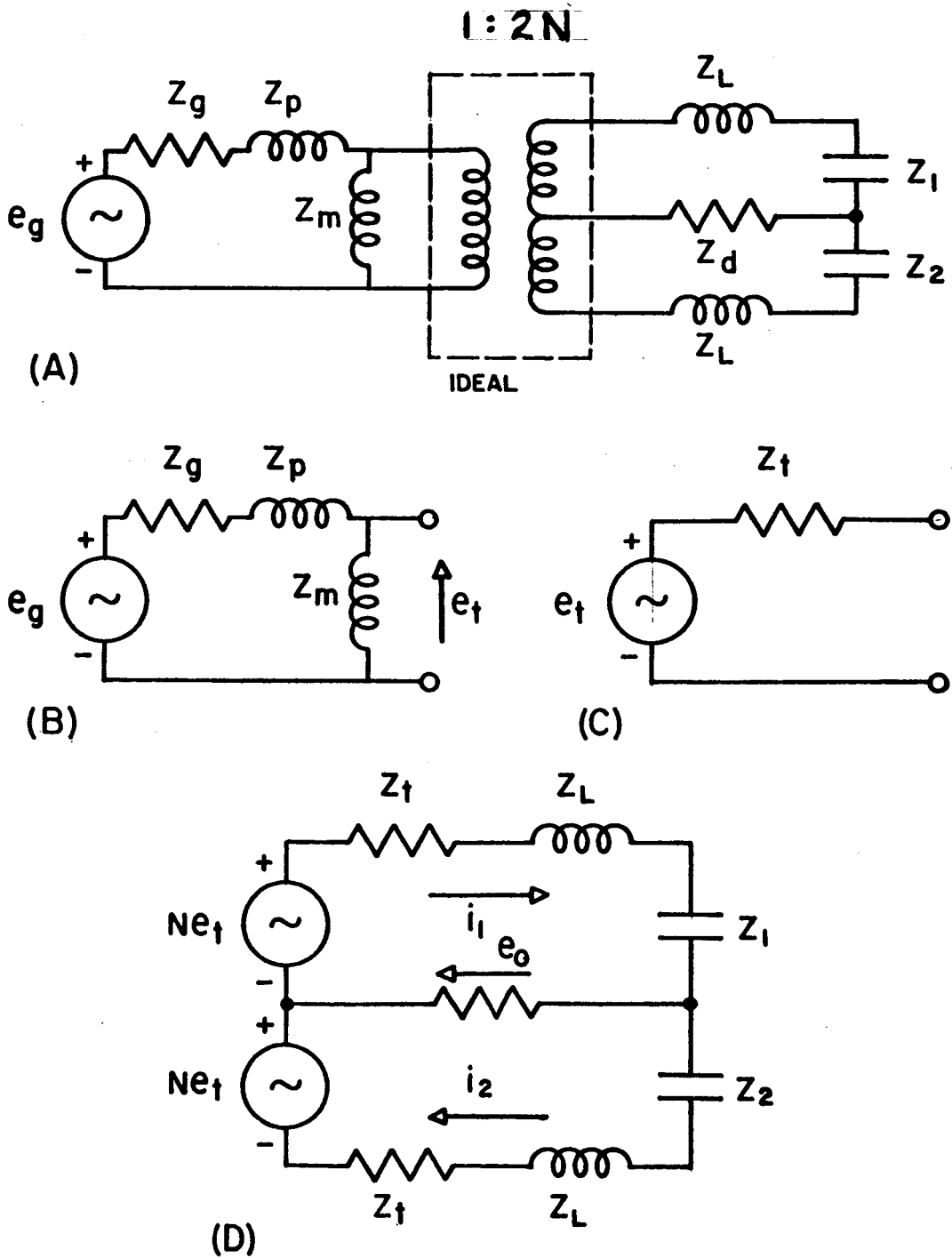
It has been found through open circuit and short circuit impedance tests that the leakage reactance of the toroidal transformer is not negligible, giving rise to a coefficient of coupling of about 0.5 . To include the effect of this leakage and the phase inversion characteristics, the practical transformer has been replaced in the analysis by an equivalent network and an ideal transformer.

The series resistance of the primary and secondary and the transformer core loss ( $Q_0 = 150$  at 54 mc/s) are neglected.

Interwinding capacitance has been reduced by using a minimum number of spaced turns on primary and secondary sides of the transformer. These measures reduced the capacitance below 4 pf., so the effects are neglected in the subsequent analysis.

The zener diodes and their bypass capacitors  $C_3$  and  $C_4$  are a.c. short circuits at the frequency of operation and therefore are not shown in the equivalent circuit.

Impedances  $Z_1$  and  $Z_2$  represent the fixed-bias and controlled-bias capacity diodes respectively.



## EQUIVALENT CIRCUITS

FIGURE 2



The Thevenin equivalent for the circuit of Figure 2B, is a generator with open circuit voltage

$$e_t = \frac{e_g Z_m}{Z_p + Z_m + Z_g} = e_g S \quad (1)$$

and an impedance

$$Z_t = \frac{Z_m (Z_g + Z_p)}{Z_p + Z_m + Z_g} = (Z_g + Z_p) S \quad (2)$$

where  $Z_m$  = magnetizing impedance

$Z_p$  = primary leakage impedance

$Z_g$  = generator impedance

$e_g$  = generator voltage

$e_t$  = equivalent Thevenin voltage

$Z_t$  = equivalent Thevenin impedance

and  $N$  = transformer turns ratio, primary to  
1/2 secondary.

From the loop equations of Figure 2D, the output voltage is

$$e_o = \frac{N e_t Z_d (Z_1 - Z_2)}{(a + Z_d + Z_1)(a + Z_d + Z_2) - Z_d^2} \quad (3)$$

where  $a = N^2 Z_t + Z_s$ .

Rearranging equation 3, the gain of the network is found to be

$$G = \frac{e_0}{e_g} = \frac{NS(Z_1 - Z_2)}{2a + Z_1 + Z_2 + Y_d(a + Z_1)(a + Z_2)} \quad (4)$$

Since "a" is a complex impedance, let

$$a = R + jX$$

Equation 4 becomes,

$$G = \frac{NS(Z_1 - Z_2)}{(2jX + Z_1 + Z_2)(1 + RY_d) + R(2 + RY_d) + Y_d(jX + Z_1)(jX + Z_2)} \quad (5)$$

The voltage controlled impedance  $Z_2$  can be expressed as follows:

$$Z_2 = -j / \omega C_2 + R$$

where  $R = 1 / \omega C_2 Q$

and  $C_2 = KV^{-n}$

giving  $Z_2 = \frac{V^n}{K\omega} (1/Q - j)$ .

Practical values of Q are greater than 10; so to a first approximation

$$Z_2 \approx -jV^n / \omega K = K' V^n \quad (6)$$

where V is the control voltage

and  $K' = -j / K\omega$ .

The bridge network gain equation 5 as a function of control voltage V, is given by

$$G = \frac{NS(Z_1 - K'V^n)}{(2jX + Z_1 + K'V^n)(1 + RY_d) + R(2 + RY_d) + Y_d(jX + Z_1)(jX + K'V^n)} \quad (7)$$

The phase shift of the attenuator may be obtained from equation 5 giving,

$$\theta = \tan^{-1}(Z_1 - Z_2) + \tan^{-1}(\text{Im}S/\text{Re}S) - \tan^{-1} \left[ \frac{(2jX + Z_1 + Z_2)(1 + RY_d)}{R(2 + RY_d) + Y_d(jX + Z_1)(jX + Z_2)} \right] \quad (8)$$

So far in this analysis it has been assumed that the diodes are identical. If this is not the case, then an additional phase shift may be produced due to the difference in their loss factors at the balance point. This effect is difficult to estimate theoretically as it is so dependent on the similarity of the capacity diode pairs employed for the bridge circuit. These differences will produce a small voltage output,  $V_o$ , at the balance point which will be approximately 90 degrees out of phase with the output voltage at the point of minimum insertion loss. The additional phase shift,  $\theta_2$ , at the point where the voltage output is  $V_m$ , is given by,  $\sin \theta \doteq V_o/V_m$ .

The effect of this additional source of phase shift can, then, simply be measured in practice by measuring the maximum attenuation which can be obtained by varying the control voltage.

### 2.1.3 NOISE

The noise contributed by the bridge attenuator to the complete system is due primarily to the back-biased capacity diodes. Noise generated by these diodes is made up of two sources, resistance noise and shot noise.

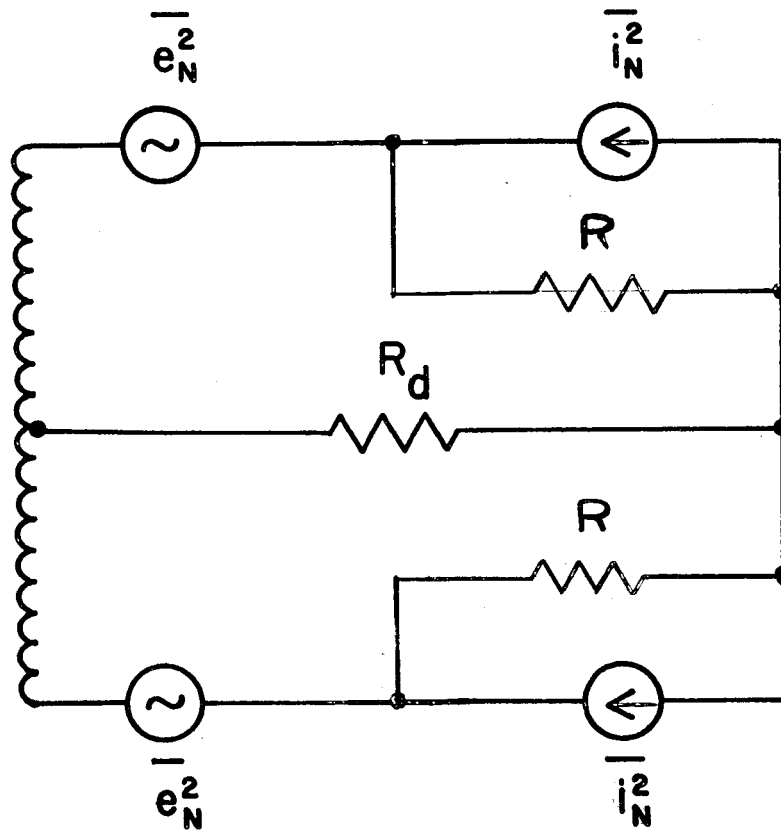
The first is a voltage source,  $\overline{e_n^2}$ , whose mean square voltage is a function of temperature and the internal series resistance of the diode.

A second noise source has an equivalent current generator, whose mean square current,  $\overline{i_n^2}$ , is proportional to the diode reverse current as it represents the shot noise for the junction.

The noise source equivalent circuit is shown in Figure 3.

Since these sources of noise are uncorrelated, their effects can be added.

The following procedure was used to obtain typical magnitudes of the noise generated by these diodes.



NOISE EQUIVALENT CIRCUIT

FIGURE 3

$$\overline{e_n^2} = 4 kTR \Delta f \quad (9)$$

$$\text{and } \overline{i_n^2} = 2qI_r \Delta f \quad (10)$$

The total mean square output noise voltage at the detector is

$$\overline{e_o^2} = 2\overline{i_n^2} R_d + 2\overline{e_n^2} \quad (11)$$

where  $k = 1.38 \times 10^{-23}$  joule/°K., Boltzman's constant

$T = 300^\circ\text{K.}$

$q = 1.6 \times 10^{-19}$  coulomb

$R = 4$  ohms, equivalent series resistance of the capacity diode

$R_d = 15,000$  ohms, maximum detector resistance

$\Delta f = 1$  kc/s, equivalent noise bandwidth

$I_r = 10^{-10}$  amp., diode reverse current at -16 volts bias.

Using the above values, equation 11 becomes,

$$\overline{e_o^2} = (9.6 \times 10^{-25} + 1.31 \times 10^{-19}) \Delta f. \quad (12)$$

Since  $\overline{i_n^2} \ll \overline{e_n^2}$  then,

$$\overline{e_o} \doteq 0.011 \mu\text{V.} \quad (13)$$

#### 2.1.4 SENSITIVITY

In order to gain some insight into the sensitivity of the circuit to control voltage, it is necessary to find the first derivative of the gain and phase with respect to the control voltage.

The second derivative of the gain equation with respect to the control voltage is of importance in determining the sensitivity of the system to parameter changes.

##### 2.1.4.1 RATE OF CHANGE OF NETWORK GAIN WITH CONTROL VOLTAGE

From equation 7,

$$G = \frac{NS(Z_1 - Z_2)}{(2jX + Z_1 + Z_2)(1 + RY_d) + R(2 + RY_d) + Y_d(jX + Z_1)(jX + Z_2)} \quad (14)$$

Let

$$\begin{aligned} A &= 1 + RY_d \\ B &= R(2 + RY_d) \\ C &= Y_d(jX + Z_1) \\ D &= 2jX + Z_1 \end{aligned}$$

equation 14 becomes,

$$G = \frac{NS(Z_1 - Z_2)}{(D + Z_2)A + B + C(jX + Z_2)} \quad (15)$$

$$\frac{\partial G}{\partial Z_2} = \frac{-NS}{(D+Z_2)A+B+C(jX+Z_2)} + \frac{-NS(Z_1-Z_2)(A+C)}{[(D+Z_2)A+B+C(jX+Z_2)]^2} \quad (16)$$

so

$$\frac{\partial G}{\partial Z_2} = \frac{-1 \{NS+G[1+Y_d(R+jX+Z_1)]\}}{(2jX+Z_1+Z_2)(1+RY_d)+R(2+RY_d)+Y_d(jX+Z_1)(jX+Z_2)} \quad (17)$$

Differentiating equation 6 with respect to control voltage gives,

$$\frac{\partial Z_2}{\partial V} = nK'V^{n-1} \quad (18)$$

The total derivative of the gain with respect to control voltage is found from the relationship,

$$\frac{dG}{dV} = \frac{\partial G}{\partial Z_2} \cdot \frac{\partial Z_2}{\partial V}$$

so

$$\frac{dG}{dV} = \frac{-nK'V^{n-1} \{NS+G[1+Y_d(R+jX+Z_1)]\}}{(2jX+Z_1+K'V^n)(1+RY_d)+R(2+RY_d)+Y_d(jX+Z_1)(jX+K'V^n)} \quad (19)$$

#### 2.1.4.2 RATE OF CHANGE OF LOGARITHMIC GAIN WITH CONTROL VOLTAGE

A useful quantity in calculating the temperature sensitivity is the rate of change of logarithmic gain with respect to control voltage.

$20 \log_{10} G = 8.68 \ln G$  so that,



$$\frac{df(G)}{dV} = 8.68 \frac{d(\ln G)}{dV} = 8.68 \frac{1}{G} \cdot \frac{dG}{dV} \quad (20)$$

Using equations 7 and 19 in equation 20 there results,

$$\frac{df(G)}{dV} = \frac{-8.68nK'V^{n-1} \{NS+G[1+Y_d(R+jX+Z_1)]\}}{NS(Z_1-K'V^n)} \quad \text{db/volt} \quad (21)$$

#### 2.1.4.3 SECOND DERIVATIVE OF LOGARITHMIC GAIN WITH RESPECT TO CONTROL VOLTAGE

Equation 21 of the preceding section is the first derivative of logarithmic gain with respect to control voltage.

Starting with this equation, let

$$E = -8.68nK'$$

$$F = 1+Y_d(R+jX+Z_1)$$

equation 21 becomes,

$$\frac{df(G)}{dV} = \frac{EV^{n-1} [NS+GF]}{NS(Z_1-K'V^n)} \quad (22)$$

Differentiating equation 22,

$$\begin{aligned} \frac{d^2f(G)}{dV^2} &= \frac{E(n-1)V^{n-2}[NS+GF]+EV^{n-1}F(dG/dV)}{NS(Z_1-K'V^n)} + \\ &\quad \frac{EV^{n-1}[N+GF][-NSnK'V^{n-1}](-1)}{[NS(Z_1-K'V^n)]^2} \end{aligned} \quad (23)$$

Rearranging equation 23,

$$\frac{d^2f(G)}{dV^2} = \frac{df(G)}{dV} \left[ \frac{n-1}{V} + \frac{nK'V^{n-1}}{Z_1 - K'V^n} \right] + \frac{dG}{dV} \left[ \frac{EFV^{n-1}}{NS(Z_1 - K'V^n)} \right] \quad (24)$$

Finally, upon substitution for the quantities E and F, equation 24 becomes,

$$\frac{d^2f(G)}{dV^2} = \frac{df(G)}{dV} \left[ \frac{n-1}{V} + \frac{nK'V^{n-1}}{Z_1 - K'V^n} \right] + \frac{dG}{dV} \left[ \frac{-8.68nK'V^{n-1}[1+Y_d(R+jX+Z_1)]}{NS(Z_1 - K'V^n)} \right] \quad (25)$$

#### 2.1.4.4 RATE OF CHANGE OF PHASE WITH CONTROL VOLTAGE

The phase sensitivity of the network can be found by taking the first derivative of the phase angle,  $\phi$ , with respect to the control voltage,  $V_c$  (V).

From equation 8,

$$\phi = \tan^{-1}(Z_1 - Z_2) + \tan^{-1} (\text{Im}S/\text{Re}S) -$$

$$\tan^{-1} \left[ \frac{2jX + Z_1 + Z_2}{R(2 + RY_d) + Y_d(jX + Z_1)(jX + Z_2)} \right] \quad (26)$$

$$\text{or } \phi = \theta + \psi - \rho \quad (27)$$

$$\text{where } \theta = \tan^{-1} (Z_1 - Z_2) \quad (28)$$

$$\psi = \tan^{-1} (\text{Im}S/\text{Re}S) \quad (29)$$

$$\rho = \tan^{-1} \left[ \frac{2jX + Z_1 + Z_2}{R(2 + RY_d) + Y_d(jX + Z_1)(jX + Z_2)} \right] \quad (30)$$

$$\text{and } S = \frac{Z_m}{Z_p + Z_m + Z_g} .$$

The derivative of the phase shift with respect to the control voltage is found from,

$$\frac{d\phi}{dV} = \frac{d\theta}{dV} + \frac{d\psi}{dV} - \frac{d\rho}{dV} \quad (31)$$

$$\text{but } \frac{d\theta}{dV} = 0$$

since  $\theta = -90$  degrees for  $Z_1 > Z_2$

and  $\theta = +90$  degrees for  $Z_1 < Z_2$  .

The quantity  $S$  is not a function of  $V$

$$\text{so, } \frac{d\psi}{dV} = 0 .$$

Equation 31 becomes,

$$\frac{d\phi}{dV} = -\frac{d\rho}{dV} = -\frac{\partial \rho}{\partial Z_2} \cdot \frac{\partial Z_2}{\partial V} \quad (32)$$

The partial derivatives will now be found. Starting with equation 30, let,

$$A = 1 + RY_d$$

$$B = R(2 + RY_d)$$

$$C = Y_d(jX + Z_1)$$

$$D = 2jX + Z_1.$$

Equation 30 becomes,

$$\rho = \tan^{-1} \left[ \frac{(D + Z_2)A}{B + C(jX + Z_2)} \right] \quad (33)$$

Differentiating equation 33,

$$\frac{\partial \rho}{\partial Z_2} = \frac{1}{1 + \left[ \frac{(D + Z_2)A}{B + C(jX + Z_2)} \right]^2} \cdot \left[ \frac{A}{B + C(jX + Z_2)} - \frac{AC(D + Z_2)}{[B + C(jX + Z_2)]^2} \right] \quad (34)$$

$$\frac{\partial \rho}{\partial Z_2} = \frac{A[B + C(jX - D)]}{[B + C(jX + Z_2)]^2 + [A(D + Z_2)]^2} \quad (35)$$

Substituting the quantities for A, B, C, and D, equation 35 becomes,

$$\frac{\partial \rho}{\partial Z_2} = \frac{(1+RY_d)[R(2+RY_d)-Y_d(jX+Z_1)^2]}{[R(2+RY_d)+Y_d(jX+Z_1)(jX+Z_2)]^2 + [(1+RY_d)(2jX+Z_1+Z_2)]^2} \quad (37)$$

Using equation 18, which is

$$\frac{\partial Z_2}{\partial V} = nK'V^{n-1}, \quad (38)$$

and equation 37 in equation 32, the result is the first derivative of the phase shift with respect to control voltage,

$$\frac{d\phi}{dV} = \frac{nK'V^{n-1}(1+RY_d)[R(2+RY_d)-Y_d(jX+Z_1)^2]}{[R(2+RY_d)+Y_d(jX+Z_1)(jX+K'V^n)]^2 + [(1+Y_d)(2jX+Z_1+K'V^n)]^2} \quad (39)$$

### 2.1.5 RELATIONSHIP OF INSERTION LOSS AND PHASE SHIFT TO THE TRANSFORMER TURNS RATIO AND SOURCE AND LOAD IMPEDANCES

#### 2.1.5.1 INSERTION LOSS

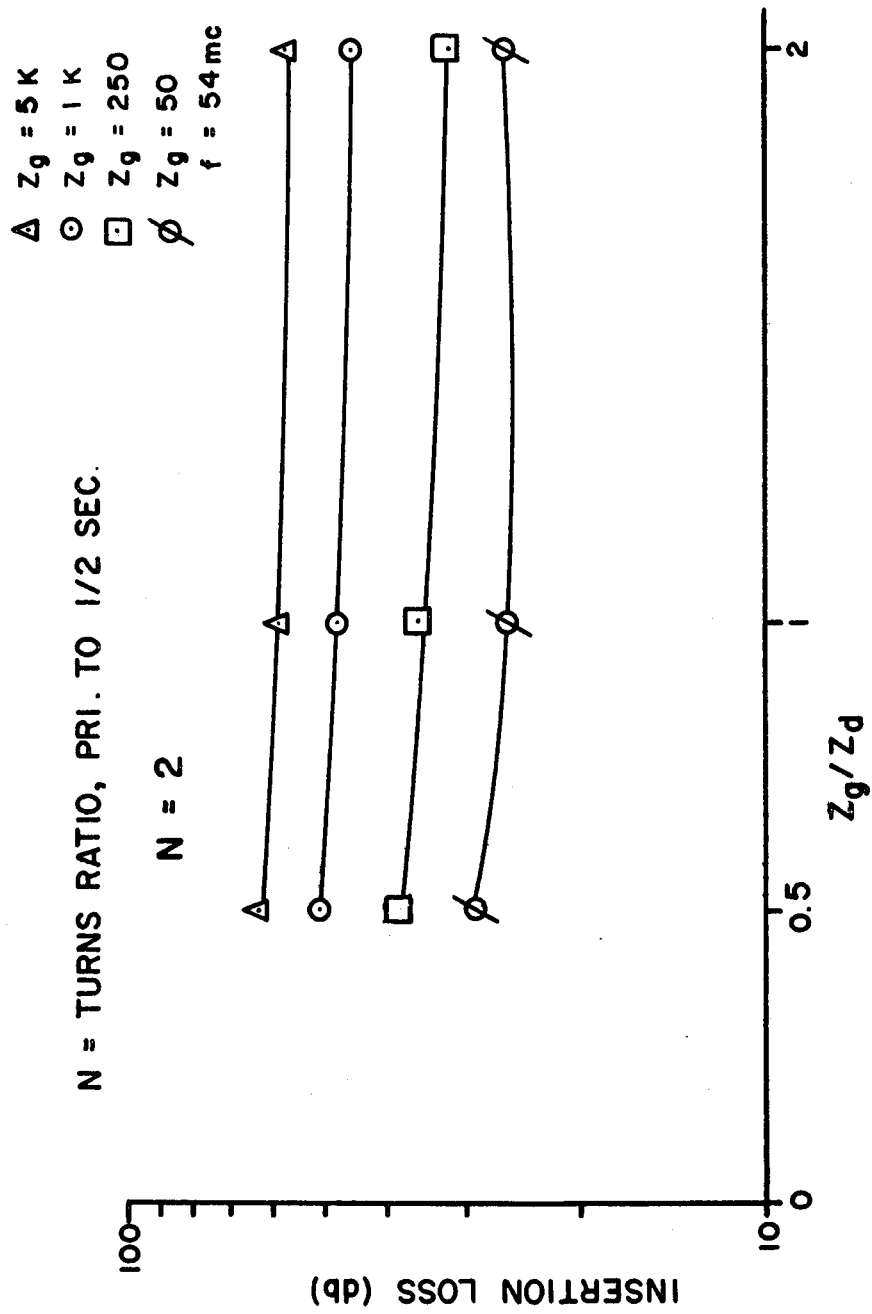
Insertion loss is defined as the ratio of the output power to the input power under conditions of minimum control (AGC) voltage. The insertion loss was investigated for three transformer ratios. Figures 4, 5, and 6 show the relationship between insertion loss and the ratio of the generator impedance ( $Z_g$ ) to the detector impedance ( $Z_d$ ) for four values of  $Z_g$ .

It can be seen for the range of variables selected the lowest insertion loss was always obtained for the smallest source impedance,  $Z_g$ , and load impedance,  $Z_d$ . In this case, these were  $Z_g = 50$  ohms and  $Z_d = 25$  ohms. The turns ratio of  $N = 1$  gave a lower insertion loss than either  $N = 0.3$  or  $N = 2$ .

The smallest insertion loss was found to be 18 db.

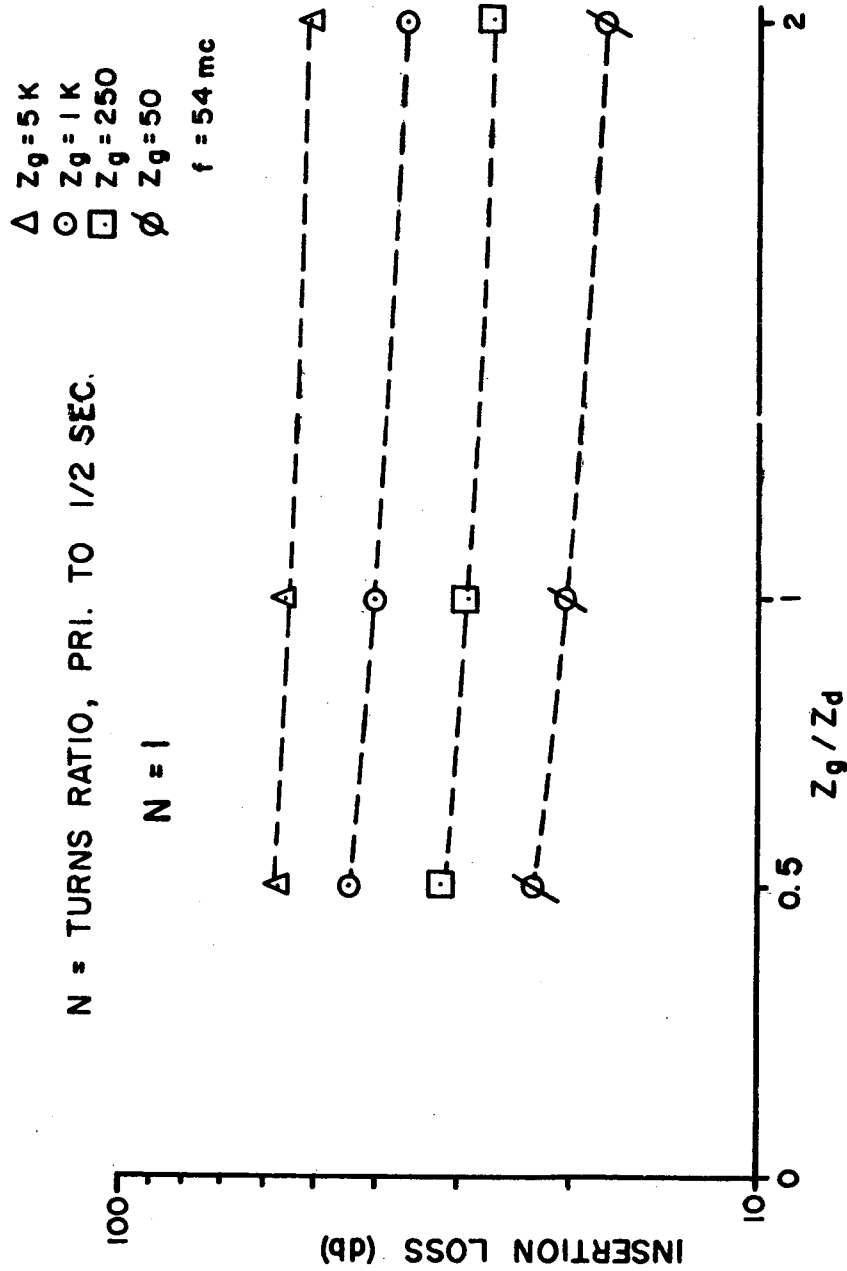
#### 2.1.5.2 OVERALL PHASE SHIFT

The overall phase shift was defined to be the change in phase when the attenuation is increased by 40 db. from the insertion loss value.



CALCULATED INSERTION LOSS VS. RATIO OF GENERATOR  
TO DETECTOR IMPEDANCE

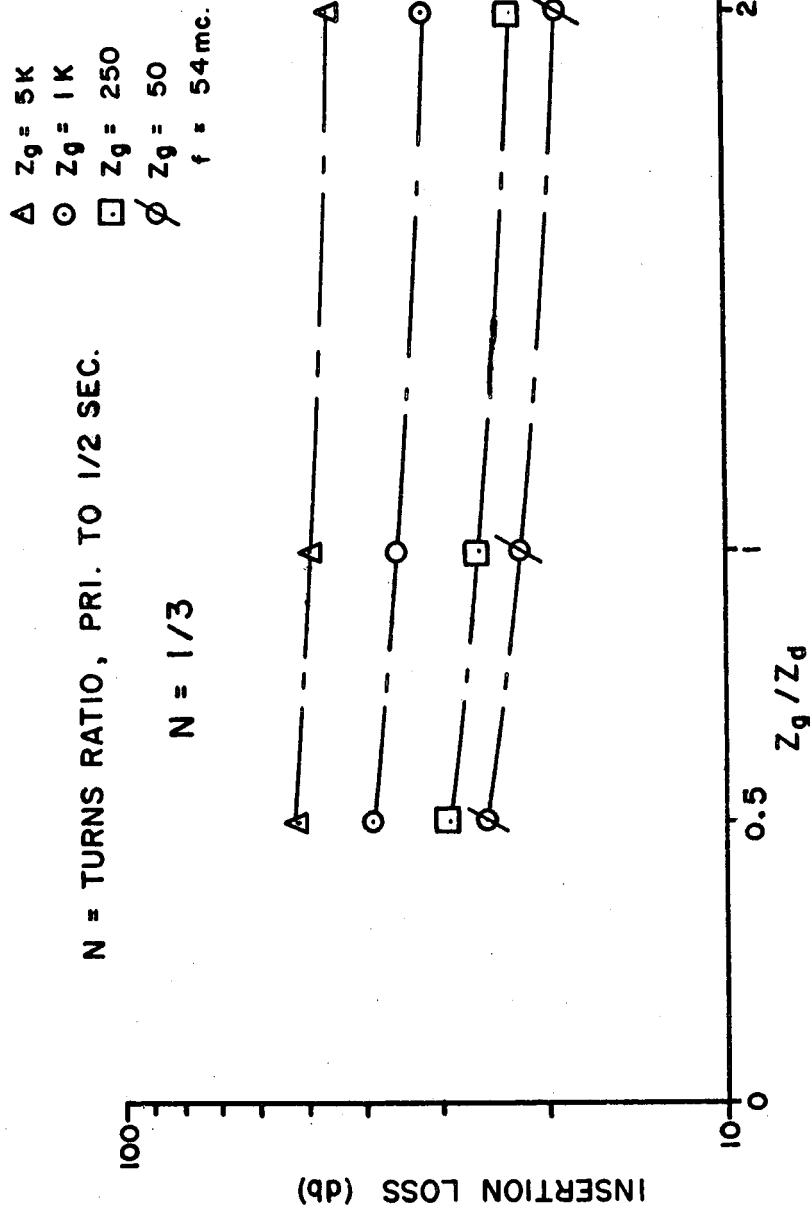
FIGURE 4



CALCULATED INSERTION LOSS VS. RATIO OF GENERATOR  
TO DETECTOR IMPEDANCE

FIGURE 5





CALCULATED INSERTION LOSS VS. RATIO OF GENERATOR  
TO DETECTOR IMPEDANCE

FIGURE 6

In Figure 7, the overall phase shifts are shown in terms of the ratio of the generator to detector impedance for the same four values of  $Z_g$  and the three transformer turns ratios.

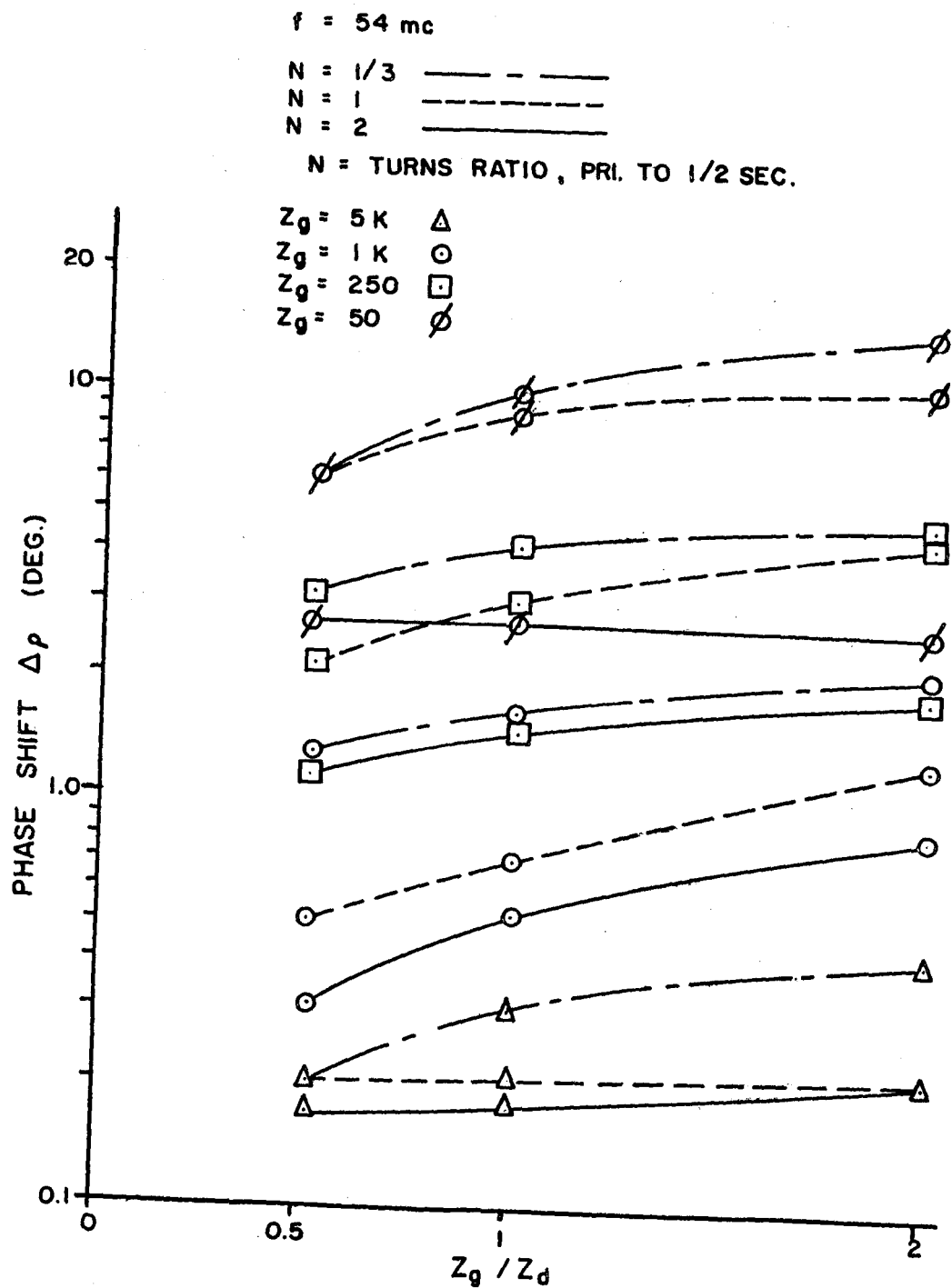
It is apparent that the conditions for lowest phase shift are quite different from those determined for lowest insertion loss.

Within the range of variables chosen, the smallest phase shift was obtained for the largest values of source impedance and load impedance. The lowest phase shift was obtained for a turns ratio  $N$  of 2.

The smallest phase shift was found to be 0.2 degrees.

#### 2.1.5.3 OPTIMUM DESIGN

It has been stated in Section 1.1, that the proposed ionospheric experiment required a system with an overall phase shift of less than  $\pm 15$  degrees, a maximum gain of 72 db. and an AGC system capable of providing a constant output within 3 db. over a dynamic range of 60 db. AGC is required over a range of 40 db. and saturation diodes may be used beyond this point.



CALCULATED CHANGE IN PHASE SHIFT VS. RATIO OF  
GENERATOR TO DETECTOR IMPEDANCE  
FIGURE 7

It is desirable to keep the total phase shift as small as possible; however, no practical purpose is served by decreasing the overall phase shift beyond about 2 degrees, the maximum resolution of the phase detector.

The criteria for smallest insertion loss and smallest phase shift are not compatible and a compromise must be made.

One such compromise might be one in which

1.  $Z_g / Z_d = 2$
2.  $Z_g = 250$  ohms, and
3.  $N = 2$  .

These parameters were chosen because for any source impedance greater than 250 ohms the insertion loss increases by at least 10 db., and for a source impedance less than 250 ohms the phase shift was greater than 2 degrees.

The ratio of  $Z_g$  to  $Z_d$  was chosen as 2, since it gave an insertion loss which was smaller by 6 db. than for  $Z_g / Z_d = 1$  and smaller by 10 db. than for  $Z_g / Z_d = 0.5$  . Lastly, the transformer turns ratio was chosen on the basis of smallest phase shift. In this case a turns ratio  $N$  of 2 produced a calculated phase shift of less than 2 degrees.

### 2.1.6 TEMPERATURE EFFECTS AND STABILITY

The temperature sensitive components used in the attenuator are the zener diodes, the capacity diodes and the bridge transformer.

#### 2.1.6.1 ZENER DIODES

One important function of the zener diodes is to ensure that under conditions of maximum AGC voltage the bridge circuit always stays on the right side of balance. In the network configuration used, zener voltage variation tends to self-compensate so that the effects of temperature on these diodes is minimized. However, to examine the "worst-case" condition it is assumed that one zener diode is ideal, the other is a practical diode and exhibits temperature sensitivity. The effect was investigated at an attenuation of 40db., for a temperature variation of  $-40^{\circ}\text{C}.$  to  $+80^{\circ}\text{C}.$

The silicon zener diodes used are temperature compensated, Motorola type 1N936A having a temperature coefficient of  $0.005\%/^{\circ}\text{C}.$ , and a zener voltage of 9 volts  $\pm 5\%$ .

The effect of voltage variation manifests itself in producing a change in capacitance of the capacity diode and therefore a change in attenuation.

The capacitance-voltage relationship for the capacity diode is given by the equation

$$C = K V^{-n} . \quad (40)$$

Implicit differentiation of equation 40 yields,

$$dC = -nK V^{-n-1} dV \quad (41)$$

Dividing equation 41 by equation 40,

$$\frac{dC}{C} = -n \frac{dV}{V} \quad (42)$$

where  $C$  = diode capacitance

$V$  = capacity diode control voltage

$K = 205 \times 10^{-12}$  farad (volts)<sup>2</sup>

$\frac{dV}{V}$  = fractional control voltage change

$\frac{dC}{C}$  = fractional VCSD capacitance change.

For a 120°C. temperature change (-40°C. to +80°C.),

$$\frac{dV}{V} = 0.6 \% \text{ or } 54 \text{ mV. (equivalent voltage change at 9 volts)} \quad (43)$$

Substitution of equation 43 in equation 42 shows

the percentage capacitance change is

$$\frac{dC}{C} = -0.265\% \text{ or } 0.16 \text{ pf. at 40 db. attenuation.} \quad (44)$$

To see the effective attenuation change ( in decibels), equation 21 is rearranged to give, (45)

$$df(G) = \frac{-8.68nK'V^n \{NS+G[1+Y_d(R+jX+Z_1)]\}}{NS(Z_1-K'V^n)} \cdot \frac{dV}{V} .$$

NUMERICAL EXAMPLE FOR OPTIMUM SYSTEM:

$$n = 0.442 \quad Z_1 = -j40.3 \text{ ohms}$$

$$K'V^n = -j39.3 \text{ ohms} \quad Z_g = 250 \text{ ohms}$$

$$N = 2 \quad Y_d = 1/125 \text{ mhos}$$

$$G = 7.63 \times 10^{-4} \quad \frac{dV}{V} = 0.006$$

Upon substituting these values, equation 45 becomes,

$$df(G) = - 151 \text{ dV/V} \quad (46)$$

$$\Delta f(G) = - 0.9 \text{ db. for a } 120^\circ\text{C. change.} \quad (47)$$

A similar procedure may be used to find the phase sensitivity of the attenuator due to temperature variation.

At an attenuation of 40 db., the change in phase is given by equation 39 which is rearranged to yield,

(48)

$$d\theta = \frac{nK'V^n(1+RY_d)[R(2+RY_d) - Y_d(jX+Z_1)] dV/V}{[R(2+RY_d)+Y_d(jX+Z_1)(jX+K'V^n)]^2 + [(1+Y_dR)(2jX+Z_1+K'V^n)]^2}$$

Using the parameter values from the previous example, the change in phase,  $\Delta\theta = 1.64 \times 10^{-2}$  degrees for a  $120^\circ\text{C.}$  change in temperature.

### 2.1.6.2 CAPACITY DIODES

Changes in temperature of the capacity diodes produces a change in attenuation and phase shift of the network.

The voltage sensitivity of the capacity diodes has been shown, in Appendix A, to be dependent upon bias level.

To examine the "worst-case" condition we assume one diode ideal and the other a practical diode. The largest temperature sensitivity occurs at a bias of 0.5 volts and is equal to 0.1%/°C. or 12%/ 120°C.

The derivative of the gain function for  $V = 0.5$  volts, however, is quite small e.g.,

for	$K'V^n = -j15.7 \text{ ohms}$	$Z_1 = -j40.3 \text{ ohms}$
	$n = 0.442$	$Z_g = 250 \text{ ohms}$
	$N = 2$	$Y_d = 1/125 \text{ mhos}$
	$G = 1.84 \times 10^{-2}$	$\frac{dV}{V} = 0.12$

equation 45 becomes,

$$df(G) = -5.93 \frac{dV}{V} \quad (49)$$

$$\Delta f(G) = -0.7 \text{ db. for a } 120^\circ\text{C. change.} \quad (50)$$

For the other case where the slope of the gain function is large (9 volts bias), the temperature coefficient of the capacity diode is,



$$(1/C)(dC/dT) = 0.008\%/^{\circ}\text{C. or } 0.98\%/120^{\circ}\text{C.}$$

Using equation 46, the change in attenuation resulting from a variation in temperature of  $120^{\circ}\text{C.}$  is

$$\Delta f(G) = -1.5 \text{ db.}$$

The phase sensitivity due to temperature effects of the capacity diode upon the network can be found by substituting the voltage sensitivities  $12\%/120^{\circ}\text{C.}$  and  $0.98\%/120^{\circ}\text{C.}$  into equation 48.

The results are the following:

1.  $\Delta \theta = 2.8 \times 10^{-1}$  degrees for  $120^{\circ}\text{C.}$  change  
at  $V = 0.5$  volts.
2.  $\Delta \theta = 2.95 \times 10^{-2}$  degrees for  $120^{\circ}\text{C.}$  change  
at  $V = 9$  volts.

## 2.2 EXPERIMENTAL PROCEDURE AND RESULTS

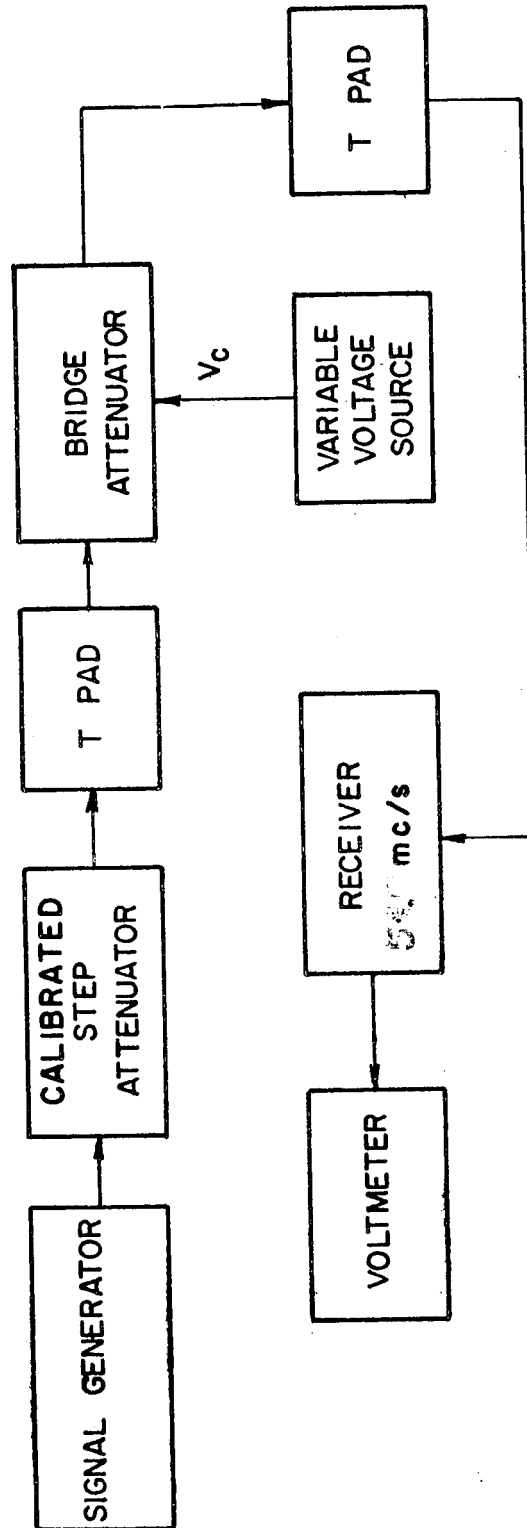
### 2.2.1 MEASUREMENT OF ATTENUATION AS A FUNCTION OF CONTROL VOLTAGE

A block diagram of the system used for the measurement of the attenuation is shown in Figure 8.

Matching "T" networks were used to control the source and load impedances for the bridge network while maintaining the proper terminating impedances for the calibrated attenuator and the receiver.

To find the attenuation as a function of control voltage, the attenuation of the bridge circuit was varied by means of the control voltage. The change of the calibrated attenuator required to provide a constant receiver output level was measured. This was equal to the change in the attenuation of the voltage controlled attenuator.

The insertion loss was found by removing the attenuator bridge and the "T" networks from the circuit and readjusting the calibrated attenuator to maintain the receiver output level constant.



BLOCK DIAGRAM FOR ATTENUATION  
MEASUREMENT AT 54 mc/s

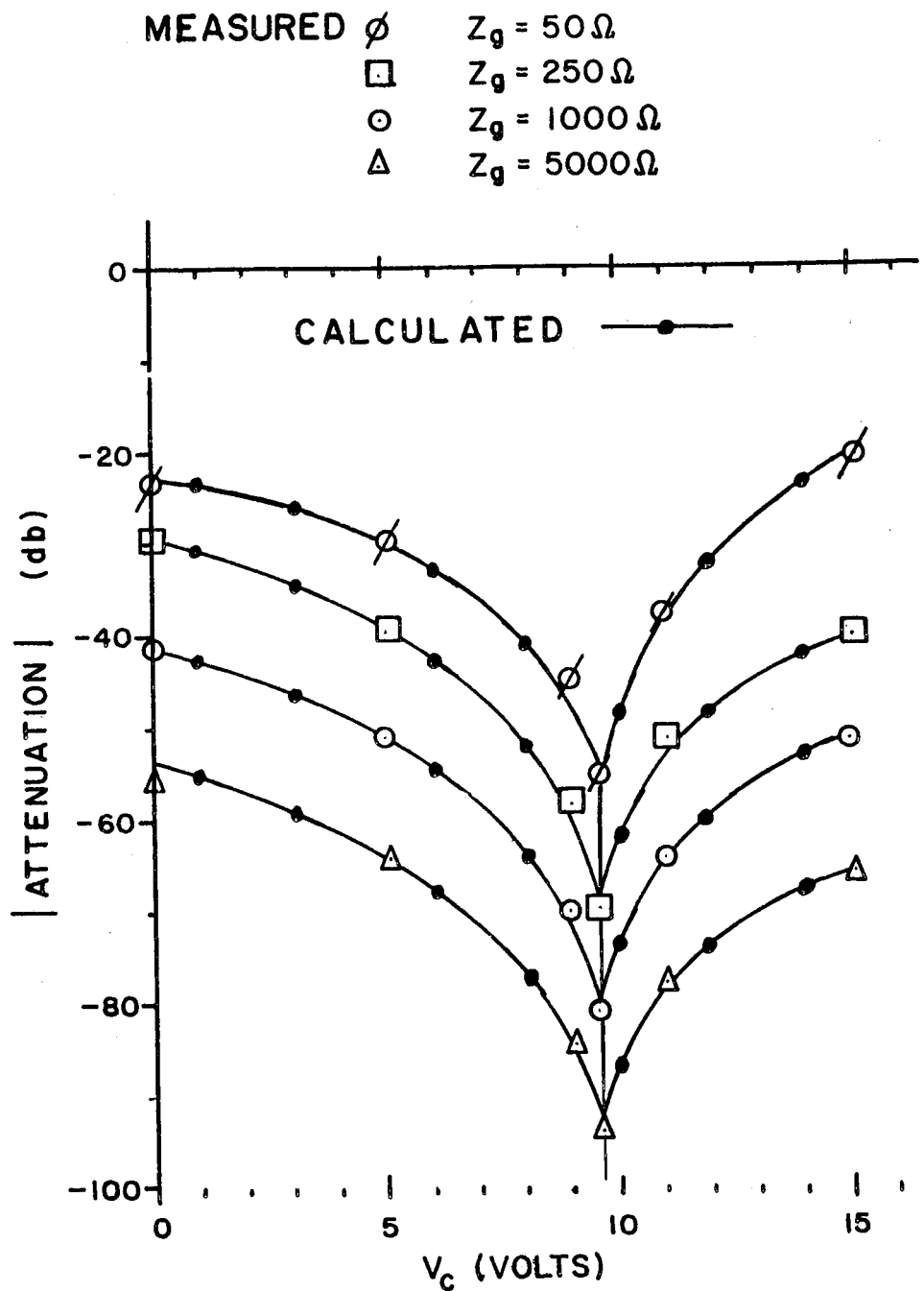
FIGURE 8

Figures 9, 10, and 11 each show, for a given transformer turns ratio, the measured and theoretical values of the network as a function of control voltage. The attenuation indicated for  $V_c$  equal to zero volts is the insertion loss.

The theoretical values were obtained using equations 6 and 15 with a digital computer.

Curves showing the attenuation characteristics have been extended beyond the balance voltage by omitting the zener diode,  $D_3$ , in Figure 1, to facilitate the comparison with the theoretical results. In practice this diode would prevent  $V_c$ , the control voltage, from exceeding the balance value of 9.5 volts.

It is apparent that the agreement between the theoretical values is within the experimental tolerances of approximately  $\pm 1$  db.

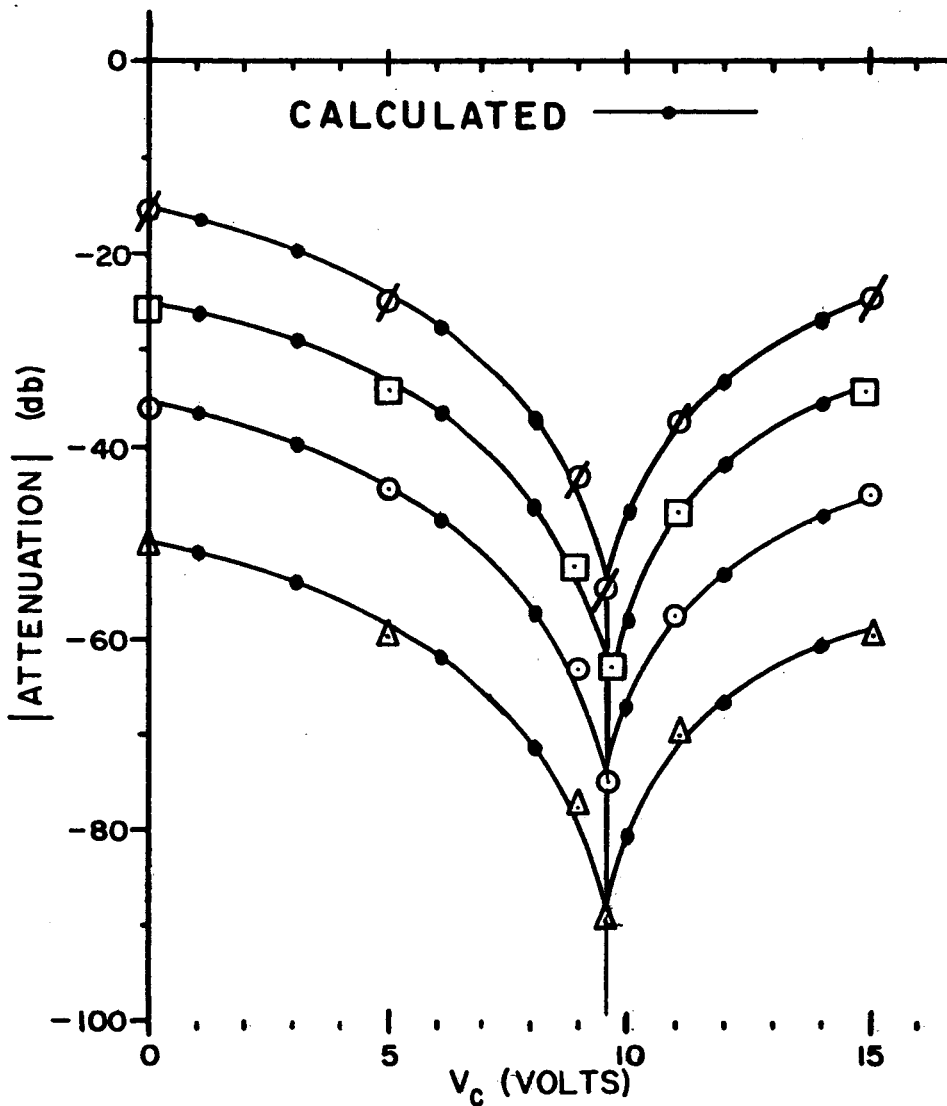


ATTENUATION VS. CONTROL VOLTAGE

FOR  $N = 2$ ,  $Z_g/Z_d = 2$

FIGURE 9

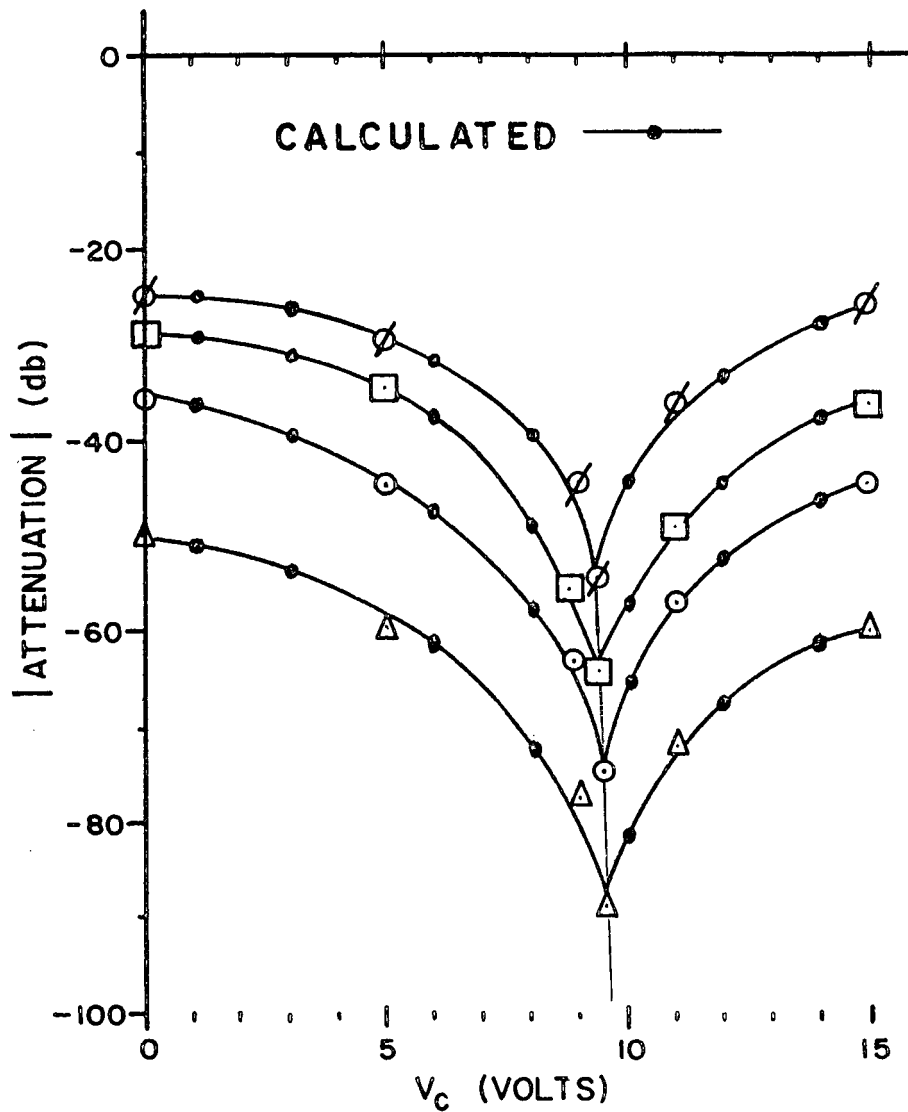
MEASURED     $\phi$   $Z = 50 \Omega$   
                   $\square$   $Z = 250 \Omega$   
                   $\circ$   $Z = 1000 \Omega$   
                   $\Delta$   $Z = 5000 \Omega$



ATTENUATION VS. CONTROL VOLTAGE  
 FOR  $N = 1$ ,  $Z_g/Z_d = 2$

FIGURE 10

MEASURED  $\phi$   $Z_g = 50 \Omega$   
 $\square$   $Z_g = 250 \Omega$   
 $\circ$   $Z_g = 1000 \Omega$   
 $\Delta$   $Z_g = 5000 \Omega$



ATTENUATION VS CONTROL VOLTAGE  
 FOR  $N = 1/3$ ,  $Z_g/Z_d = 2$

FIGURE 11

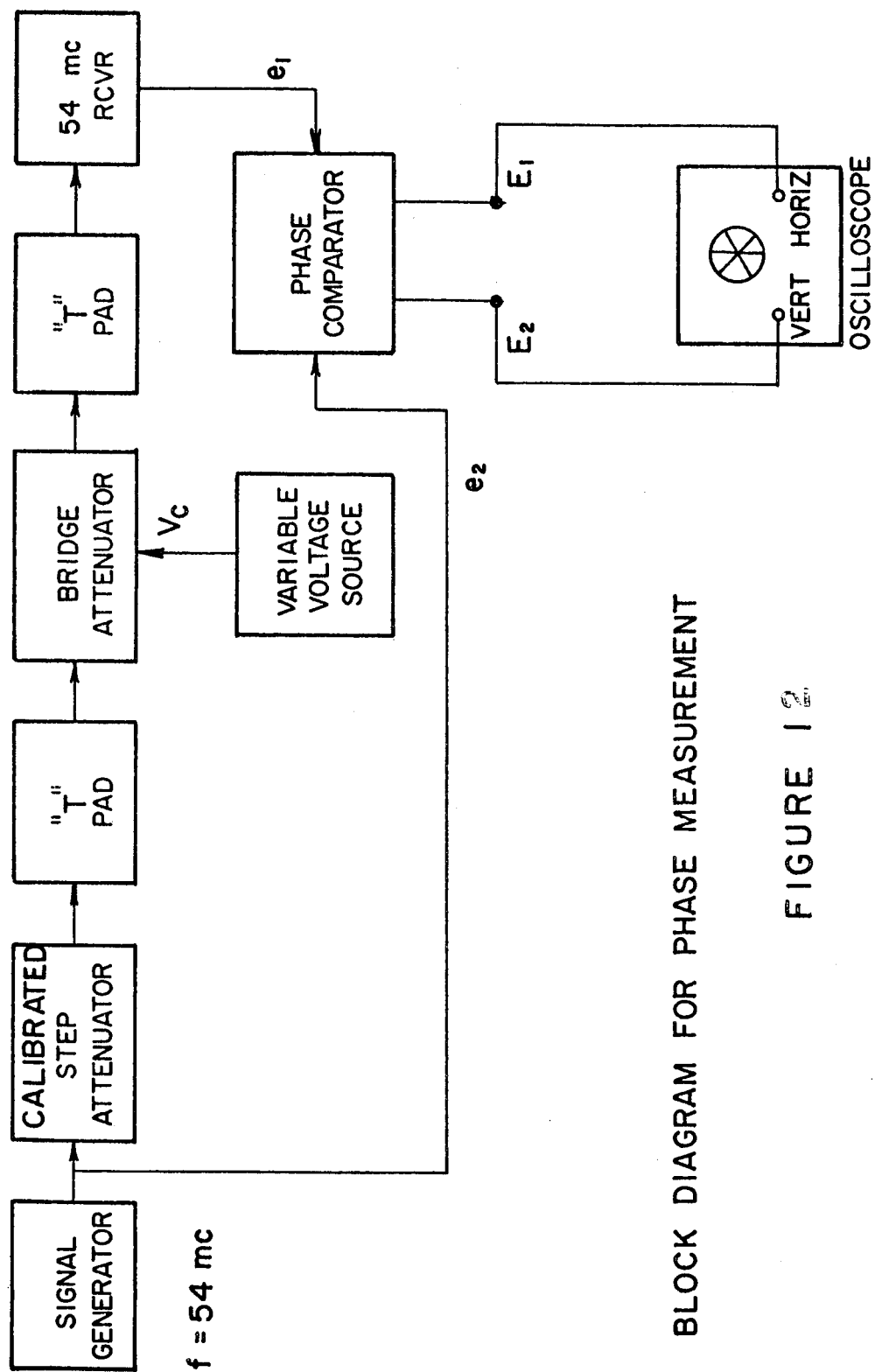
### 2.2.2 OVERALL PHASE SHIFT MEASUREMENT

Because of the very small phase shifts introduced by a suitably designed bridge attenuator, great care had to be taken in the method of phase measurement.

It was found, for example, that the receiver phase shift was amplitude dependent. Because of these effects it was decided to employ the system shown in Figure 12. In this system the difference in phase is measured between two points on either side of the balance point at which the attenuation is the same. In this way the signal levels in all parts of the circuit are the same. This difference in phase shift can then be compared with the theoretical calculations to verify the correctness of the theory.

The phase comparator used is described in detail in Appendix B. The phase resolution of this measuring system is  $\pm 3$  degrees at 54mc/s.





BLOCK DIAGRAM FOR PHASE MEASUREMENT

FIGURE 12

The phase shift measurements were made for a generator with twice the detector impedance, since in the optimum system this ratio was used.

Comparison between the theoretical and the measured values of overall phase shift are shown in Table 1.

TABLE 1

Source Impedance $Z_g$ (ohms)	Load Impedance $Z_d$ (ohms)	Turns Ratio N	Calculated Phase Shift $\Delta\theta_c$ (deg.)	Measured Phase Shift $\Delta\theta_m$ (deg.)
50	25	2	183	186 $\pm$ 3
250	125	2	182	183 $\pm$ 3
1000	500	2	180.8	180 $\pm$ 3
5000	2500	2	180.2	180 $\pm$ 3
50	25	1	190	192 $\pm$ 3
250	125	1	184	183 $\pm$ 3
1000	500	1	181	183 $\pm$ 3
5000	2500	1	180.2	180 $\pm$ 3
50	25	0.3	194	189 $\pm$ 3
250	125	0.3	185	186 $\pm$ 3
1000	500	0.3	181.8	186 $\pm$ 3
5000	2500	0.3	180.3	180 $\pm$ 3

### 2.2.3 OPTIMUM SYSTEM PERFORMANCE TESTS

Figure 13 shows attenuation as a function of control voltage for the optimum system given in Section 2.1.5.3. The measured value of 30 db.insertion loss for the case when  $V_c = 0$  volts, was obtained in agreement with the theoretical value. Up to 40db. additional attenuation, the theoretical and measured values were within the experimental tolerance of  $\pm 1$  db. Close to the bridge balance value of  $V_c = 9.5$  volts, it is noted that the rate of change of attenuation with control voltage is very large and in practice it was not found possible to make accurate measurements within 1/2 volt of this point.

Figure 14 is a graph of the overall phase shift as a function of control voltage for the optimum system. Due to the measuring technique and the  $\pm 3$  degrees phase resolution of the phase measuring system, a single value of measured phase change is shown which describes the overall phase shift found using the method outlined in Section 2.2.2 . It can be seen from Figure 15 that the rate of change of phase shift is greatest for small values of control voltage. The theoretical values for the phase shift were calculated using equations 8 and 39. It was noted in Section 2.1.2 that unbalance in the capacity diodes may produce an extra phase shift in the region of maximum attenuation. Because of the

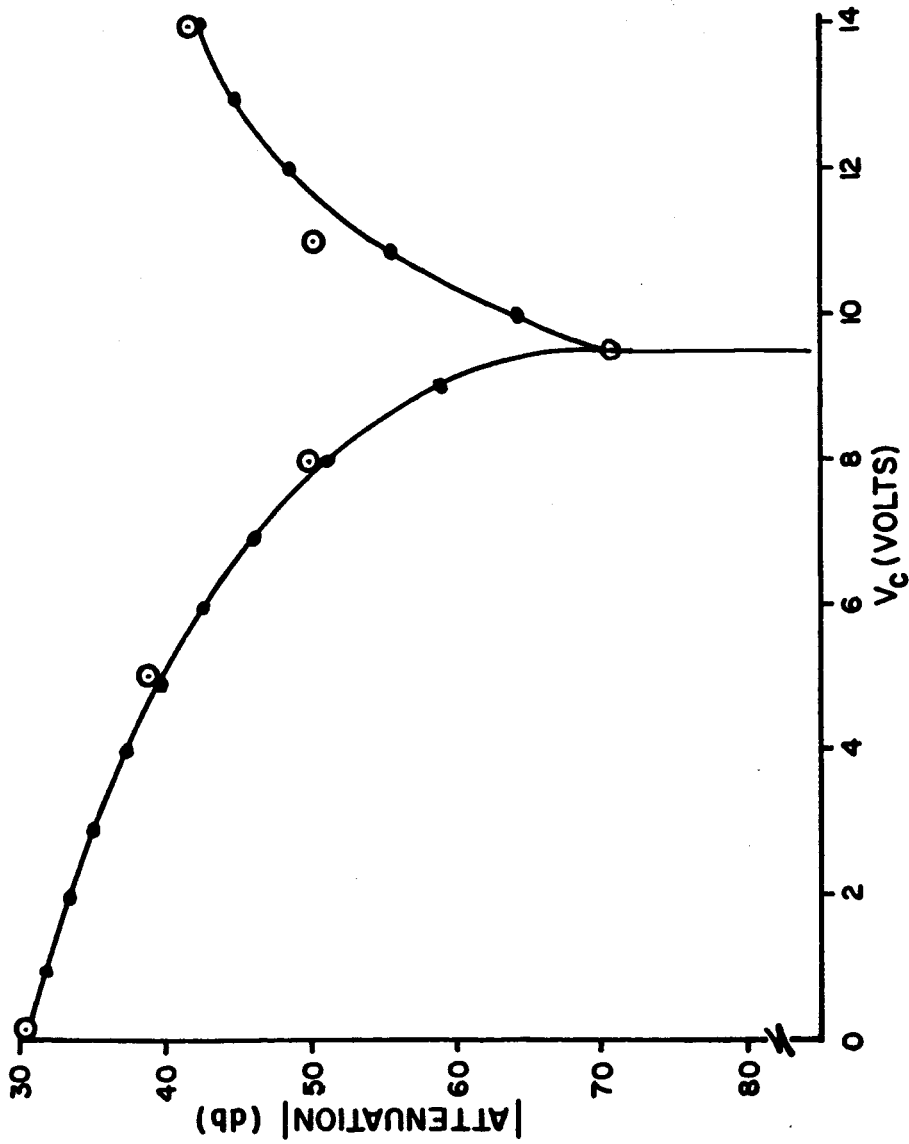
—●— CALCULATED  
○ MEASURED

$z_g = 250 \Omega$

$z_d = 125 \Omega$

$N = 2$

$f = 54 \text{ mc/s}$



ATTENUATION VS CONTROL VOLTAGE

FIGURE 13

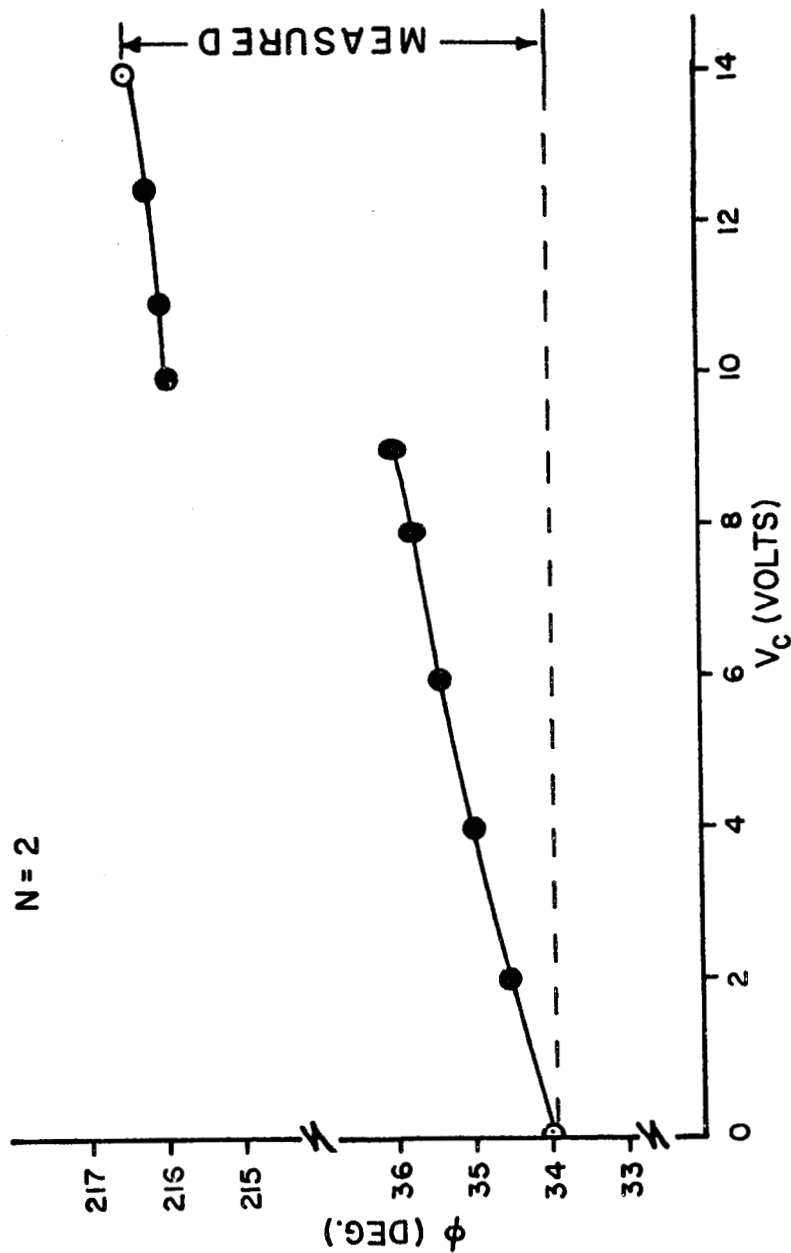
—●— CALCULATED

$z_g = 250 \Omega$

$z_d = 125 \Omega$

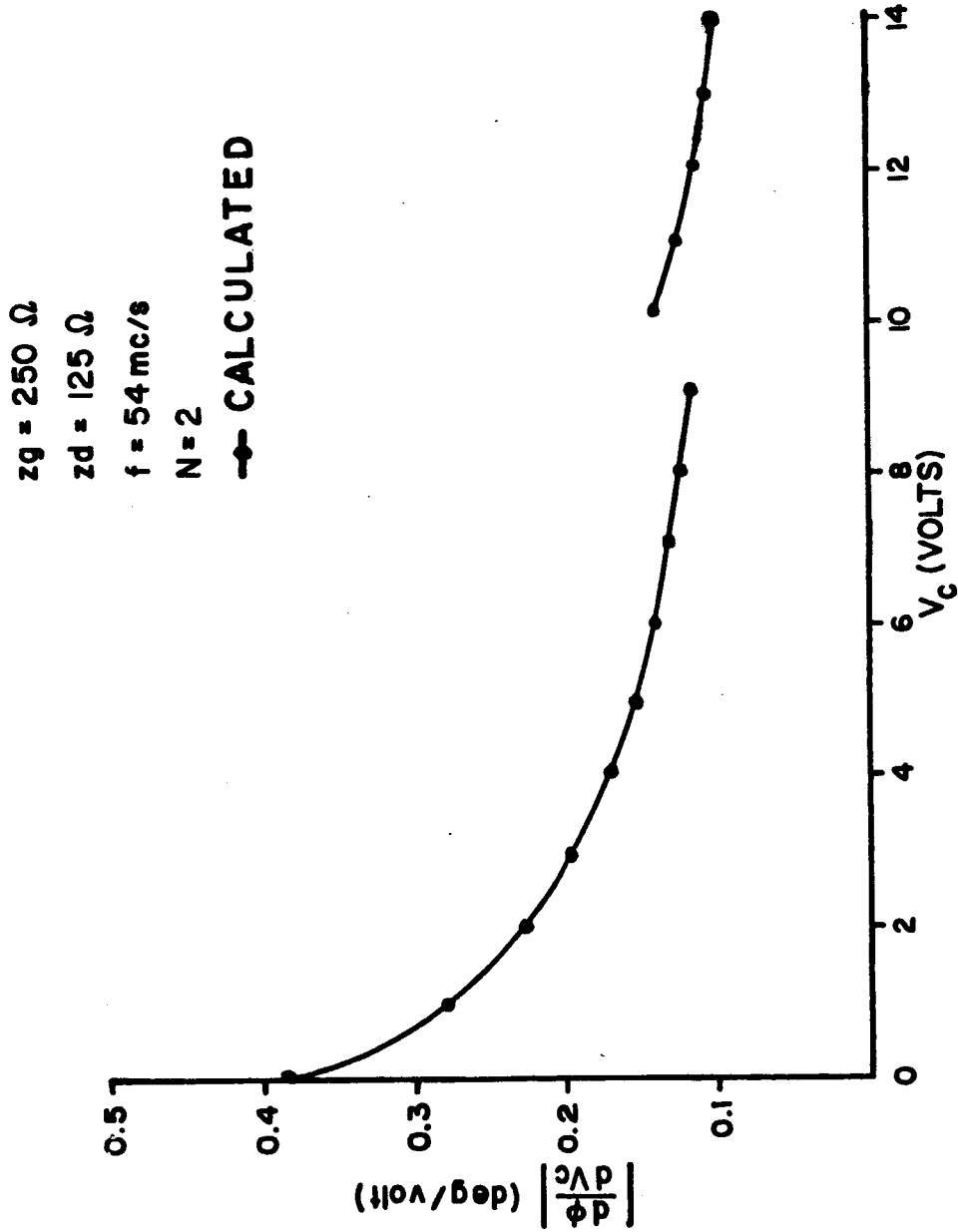
$f = 54 \text{ mc/s}$

$N = 2$



PHASE VS CONTROL VOLTAGE

FIGURE 14



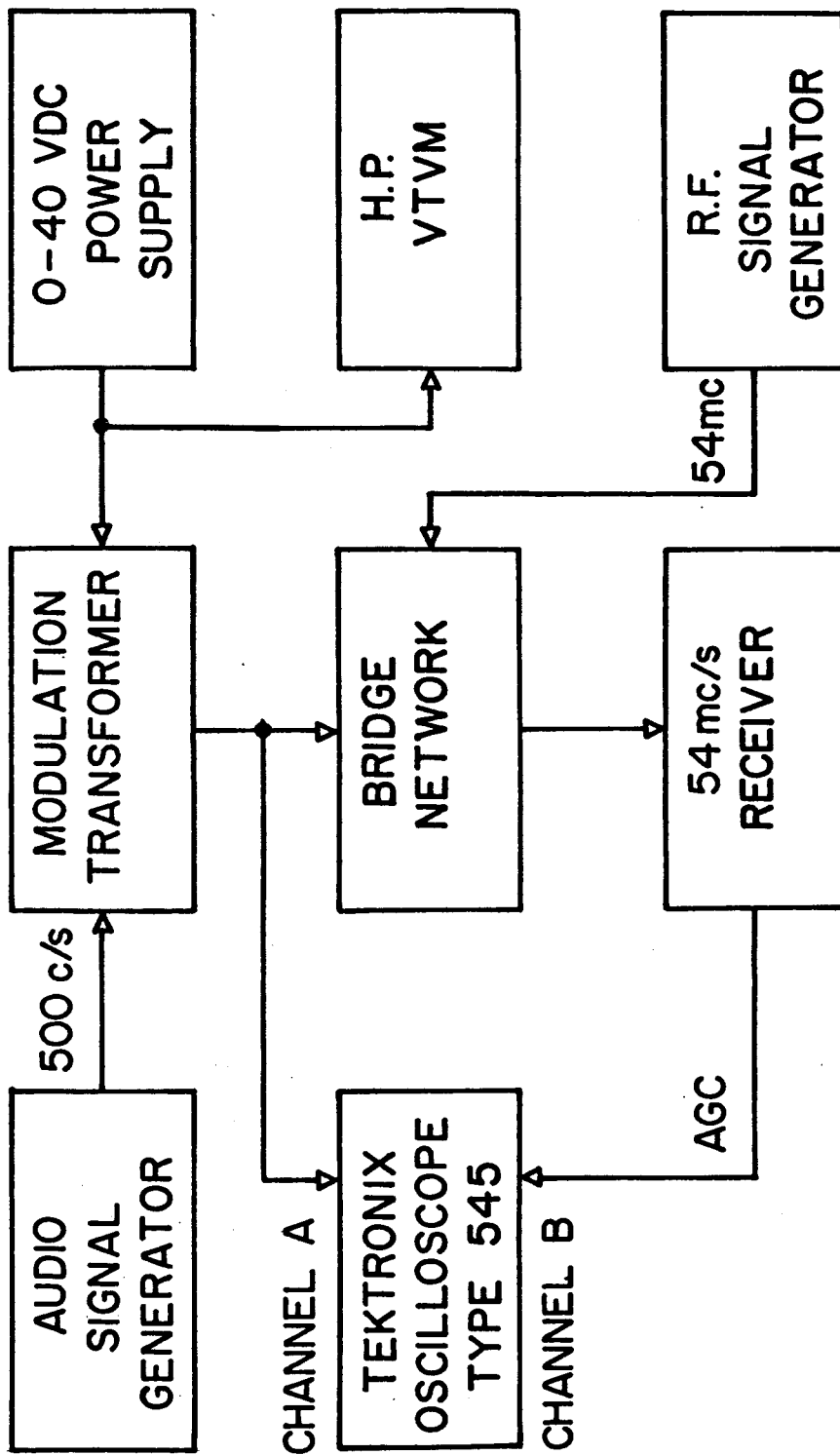
DERIVATIVE OF PHASE VS CONTROL VOLTAGE

FIGURE 15

low levels involved it was not found possible to make accurate phase measurements in this region and instead the relation between the maximum attenuation and phase shift given on Page 14 was used.

With a typical pair of silicon diodes a maximum attenuation of 63db. above the insertion loss value was obtained. This corresponds to a voltage ratio at the 40db. point of 14.1 and a phase shift of 4.1 degrees. By choosing matched diodes this phase angle could be reduced by at least a factor of 4.

Figure 16 is the block diagram for the measurement of the derivative of the attenuation with respect to the control voltage. In this test the control voltage was modulated at a frequency of 500c/s. This frequency was chosen to be low enough to be within the I.F. and AGC bandpass limits of the receiver. The modulated receiver AGC voltage is proportional to the slope of the bridge attenuation curve about any point chosen by  $V_c$ , provided the R.F. input level to the receiver is constant. In Figure 17, the rate of



BLOCK DIAGRAM FOR DERIVATIVE MEASUREMENT

FIGURE 16



—●— CALCULATED  
 ○ MEASURED

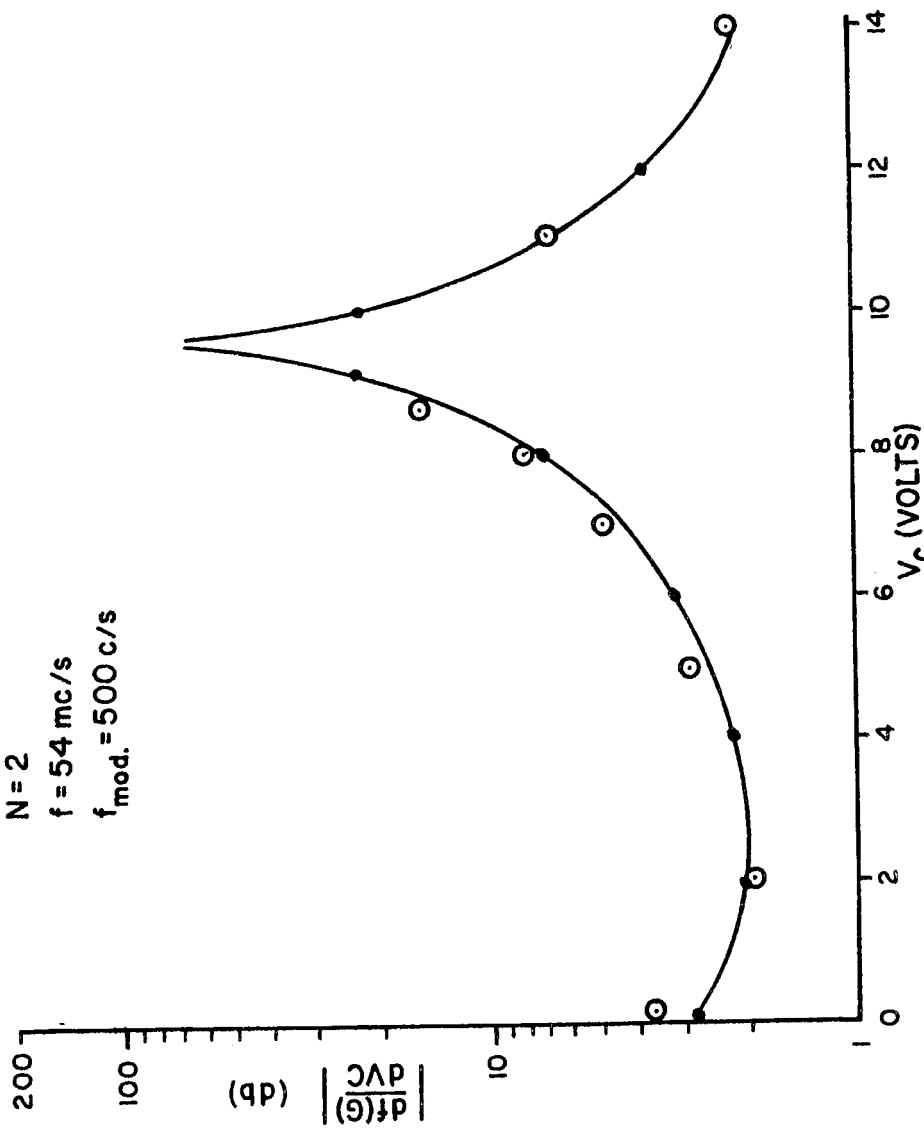
$z_g = 250 \Omega$

$z_d = 125 \Omega$

$N = 2$

$f = 54 \text{ mc/s}$

$f_{\text{mod.}} = 500 \text{ c/s}$

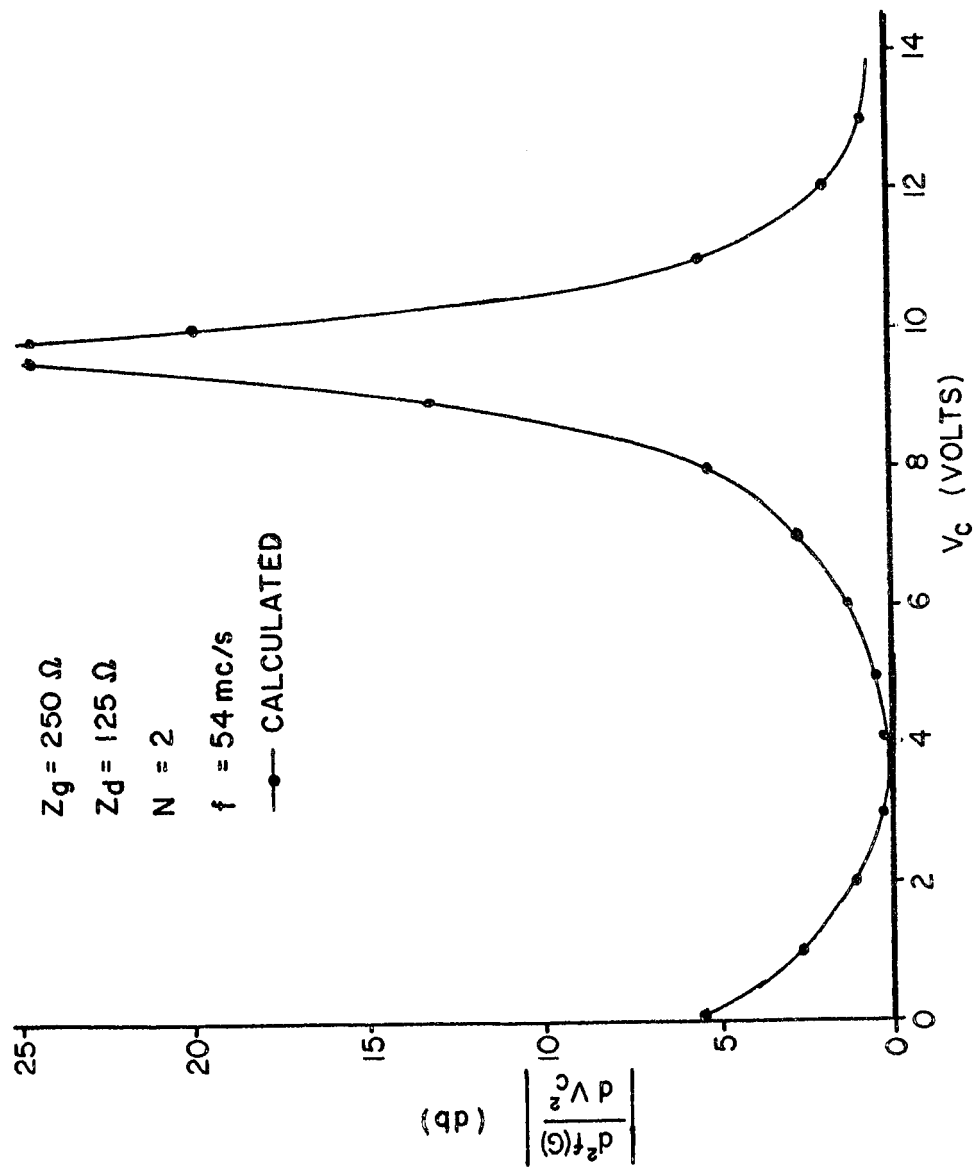


FIRST DERIVATIVE OF ATTENUATION VS CONTROL VOLTAGE

FIGURE 17

change of attenuation is shown as a function of control voltage. The theoretical values were obtained using equation 21 and the parameters of the network selected in Section 2.1.5.3 . It is apparent that the measured and theoretical values are in good agreement.

The theoretical values for the second derivative of the attenuation with respect to control voltage have been calculated using equation 25 and are shown in the graph of Figure 18. This figure has been included for convenience in determining the slope of the first derivative; no measurement was made.



SECOND DERIVATIVE OF ATTENUATION VS. CONTROL VOLTAGE  
FIGURE 18

#### 2.2.4 TEMPERATURE MEASUREMENTS

Since the bridge attenuator is to be a part of a rocket payload, a temperature range of  $-40^{\circ}\text{C.}$  to  $+80^{\circ}\text{C.}$ , which exceeds the payload test specifications, was used for the measurements.

##### 2.2.4.1 CAPACITY DIODE

The temperature test for a typical V-100 Varicap diode (VSCD) was conducted using the system shown in the block diagram of Figure 19A.

The quantity of interest in this measurement is the temperature coefficient because it is this term that is used in calculating the attenuation and phase sensitivities. Figure 20 shows the comparison of the theoretical and measured temperature coefficients as a function of control voltage for the same typical capacity diode.

##### 2.2.4.2 BRIDGE TRANSFORMER

A block diagram for the transformer temperature test is shown in Figure 19B. The results of this test yield the following temperature sensitivities:

For  $Q_0 = \omega L / R_s$  at 25mc/s

$$\Delta Q_0 = 0.076\% / ^{\circ}\text{C.}$$

$$\Delta L = 0.039\% / ^{\circ}\text{C.}$$

$$\Delta R_s = 0.12\% / ^{\circ}\text{C.}$$

The transformer parameters as a function of temperature are shown in Figure 21.

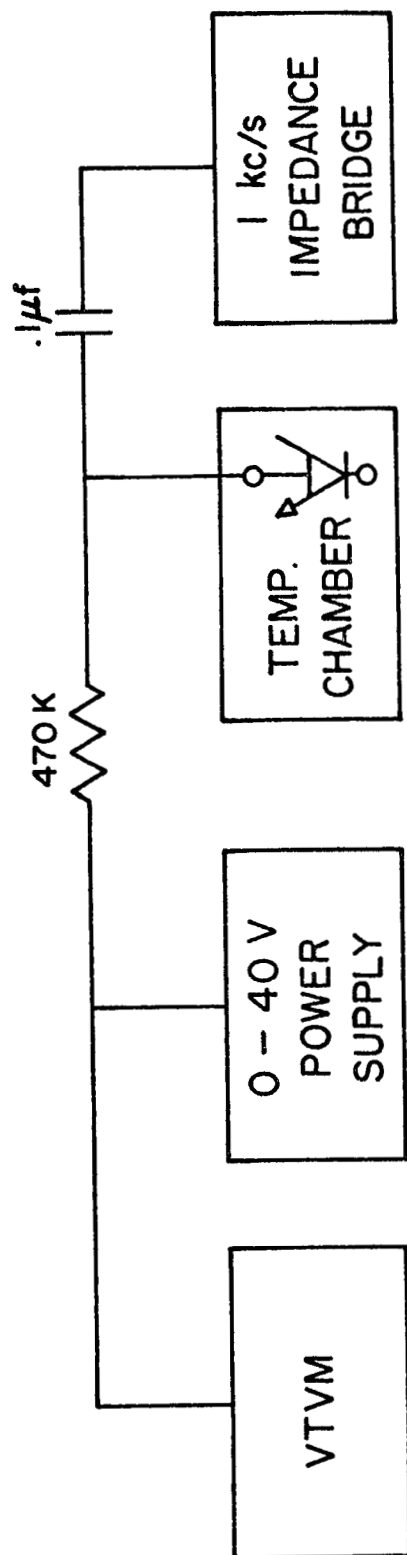


FIGURE 19 A

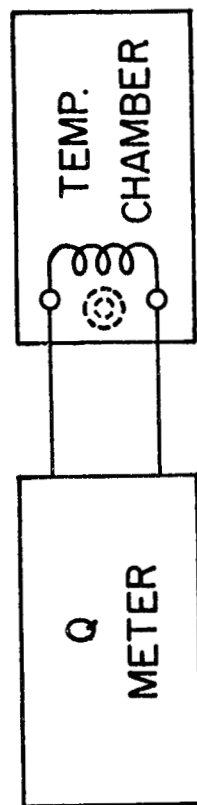
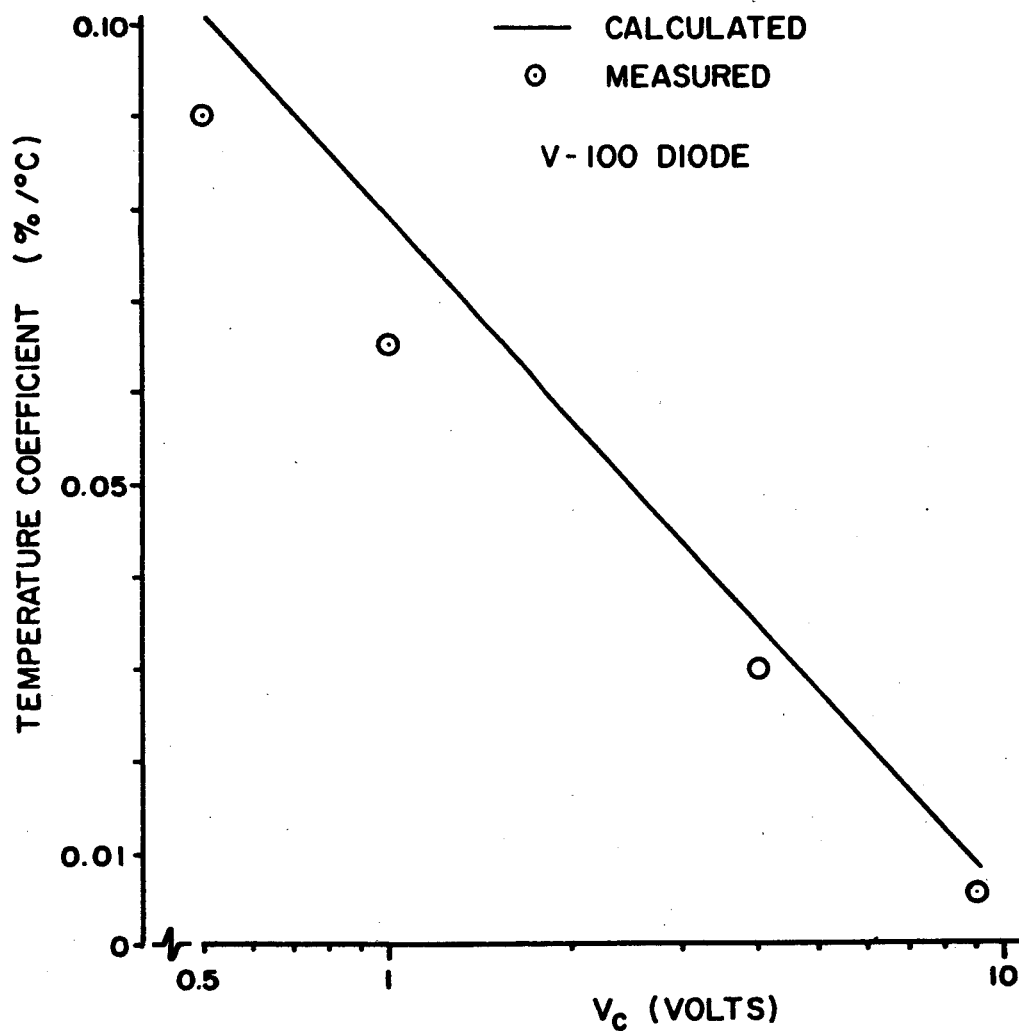


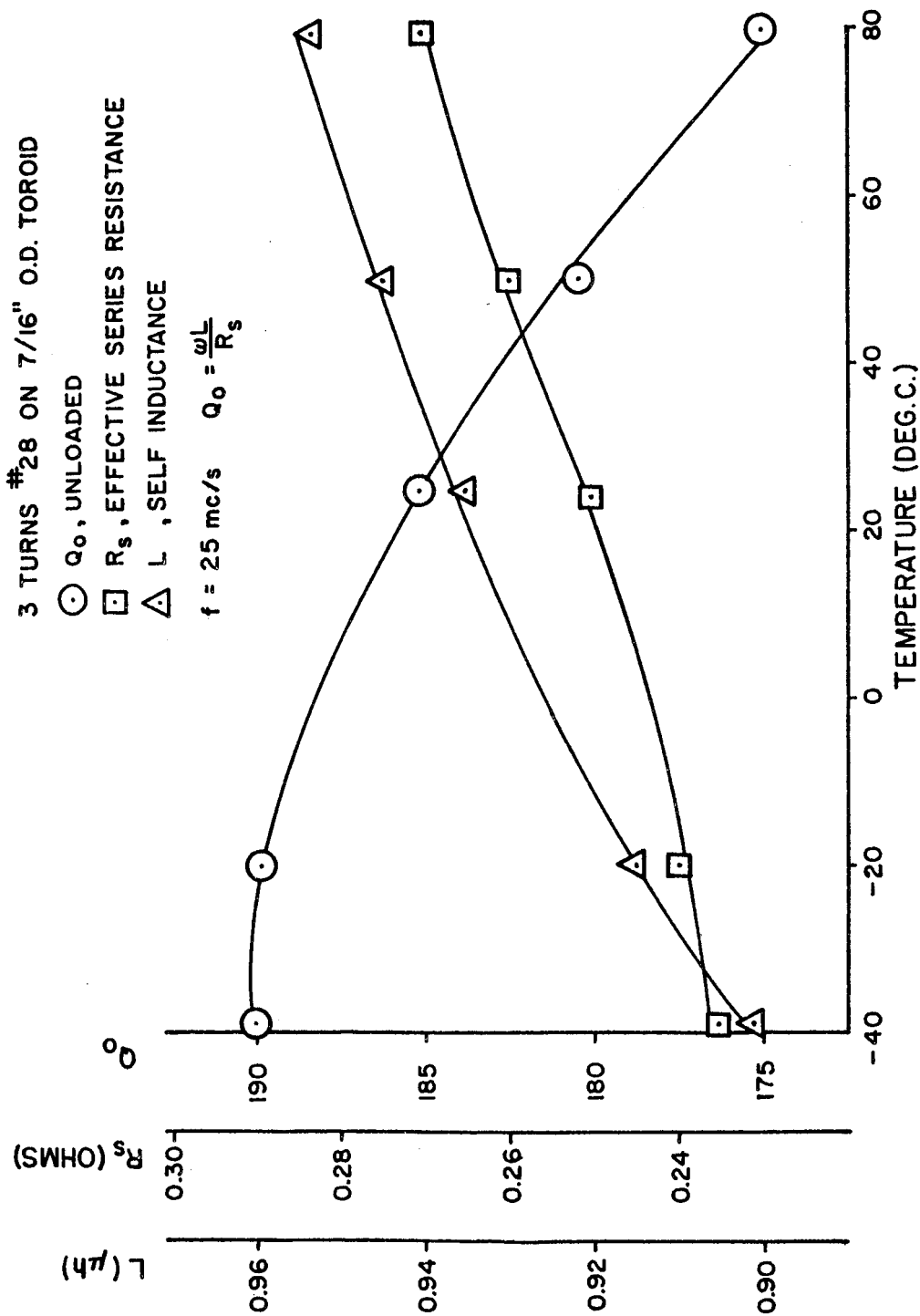
FIGURE 19 B

## BLOCK DIAGRAM FOR TEMPERATURE TESTS



V S C D TEMPERATURE COEFFICIENT  
VS. CONTROL VOLTAGE

FIGURE 20



TRANSFORMER PARAMETERS VS. TEMPERATURE

FIGURE 21

Since  $Q_0$  is on the order of 185 at 25mc/s and 55 at 72mc/s for  $T = 26^\circ\text{C}$ .,  $R_s \ll \omega L$  and therefore the variation of the effective series resistance with temperature can be neglected.

The total change in inductance is 4.7% for a  $120^\circ\text{C}$ . variation. Using equations 4 and 8, it is found that the resultant change in attenuation is 0.1 db., while the change in phase is  $1.2 \times 10^{-2}$  degrees produced by temperature effects on the bridge transformer.

#### 2.2.4.3 COMPLETE ATTENUATOR SYSTEM

Temperature cycling the entire bridge attenuator network over the  $120^\circ\text{C}$ . range reveals the following:

1. The measured change of attenuation at a control voltage of 9 volts (-40 db.) was -2.7 db. The calculated change of attenuation consisted of two sources; -0.9db. due to zener diode temperature effects and -1.5db. predicted from temperature considerations of the capacity diode. The total calculated change, then, was -2.4db.
2. For a control voltage of 0.5 volts (0db.), the calculated change of attenuation was -0.7 db.; No change in attenuation was observed in the temperature test.

The experimental accuracy for this experiment was  $\pm 1\text{db}$ .



### 3. SUMMARY AND CONCLUSIONS

A voltage controlled attenuator was analyzed to determine the relation between the control voltage and the attenuation and phase shift.

The factors which affect the relationship of the insertion loss and phase shift were investigated. It was found that the minimum phase shift and minimum insertion loss were not obtained for the same parameters. Within the range investigated, it was found that the minimum insertion loss was obtained for the smallest source and load impedances and a transformer turns ratio of one. The lowest insertion loss for an input impedance of 50 ohms and a load impedance of 25 ohms was 18 db. Under these conditions the phase shift was calculated to be 10 degrees.

The smallest phase shift was found to be obtained for the largest source and load impedances in the range and for a turns ratio of 2. The smallest phase shift for an input impedance of 5000 ohms and a load impedance of 2500 ohms was found to be 0.2 degrees. However, under these conditions the insertion loss was 55 db.

It was therefore necessary to select an optimum configuration to obtain reasonable values of insertion loss without degrading the phase characteristics of the overall system. The optimum system chosen had an input impedance of 250 ohms , a load impedance of 125 ohms and a turns ratio of 2. With these values an overall phase shift of 2 degrees for a 40 db. change in attenuation was obtained with an insertion loss of 30 db.

The temperature characteristics of the circuit were investigated. The network sensitivity to changes in control voltage was determined first; then, the changes in control voltage were found in terms of the temperature coefficients for the zener diodes and the capacity diodes.

It was found theoretically that the major sources of variation were the temperature coefficients of the zener diodes and the capacity diodes. For the optimum system these collectively produced a 2.4 db. change in attenuation as the temperature was changed from  $-40^{\circ}\text{C}.$  to  $+80^{\circ}\text{C}.$  Of this change it was found that 1.5 db. was due to the

capacity diodes and 0.9 db. was due to the zener diodes. A practical measurement on a complete circuit showed a total attenuation shift of  $2.7 \pm 1$  db.

The optimum system may be compared with that described by Hurtig (1955) in which the attenuation was controlled by a diode external to the transistor. If we assume the same receiver bandwidth of 1.4mc/s, the voltage controlled bridge attenuator would produce a center frequency shift of 93c/s compared with the value of 72kc/s obtained by Hurtig. With the bridge network the bandwidth would be effectively unchanged, since it is untuned, whereas the circuit by Hurtig produced a 40kc/s variation for a similar change of attenuation.

Seliga (1961) has shown, in his discussion of forward and reverse AGC, a phase shift of 70 degrees for reverse AGC and a 60 degree phase shift for forward AGC occurs in an 11mc/s amplifier for a 30 db. change of attenuation. In comparison, the bridge attenuator would produce a 3.2 degree phase shift for a 30 db. change of attenuation.

APPENDIX A

THE VOLTAGE SENSITIVE CAPACITY DIODE

A1. VOLTAGE SENSITIVITY

The voltage sensitivity of a PN junction diode usually follows the power relationship  $C = K/(V_c + V_b)^n$ , where K is the constant of proportionality

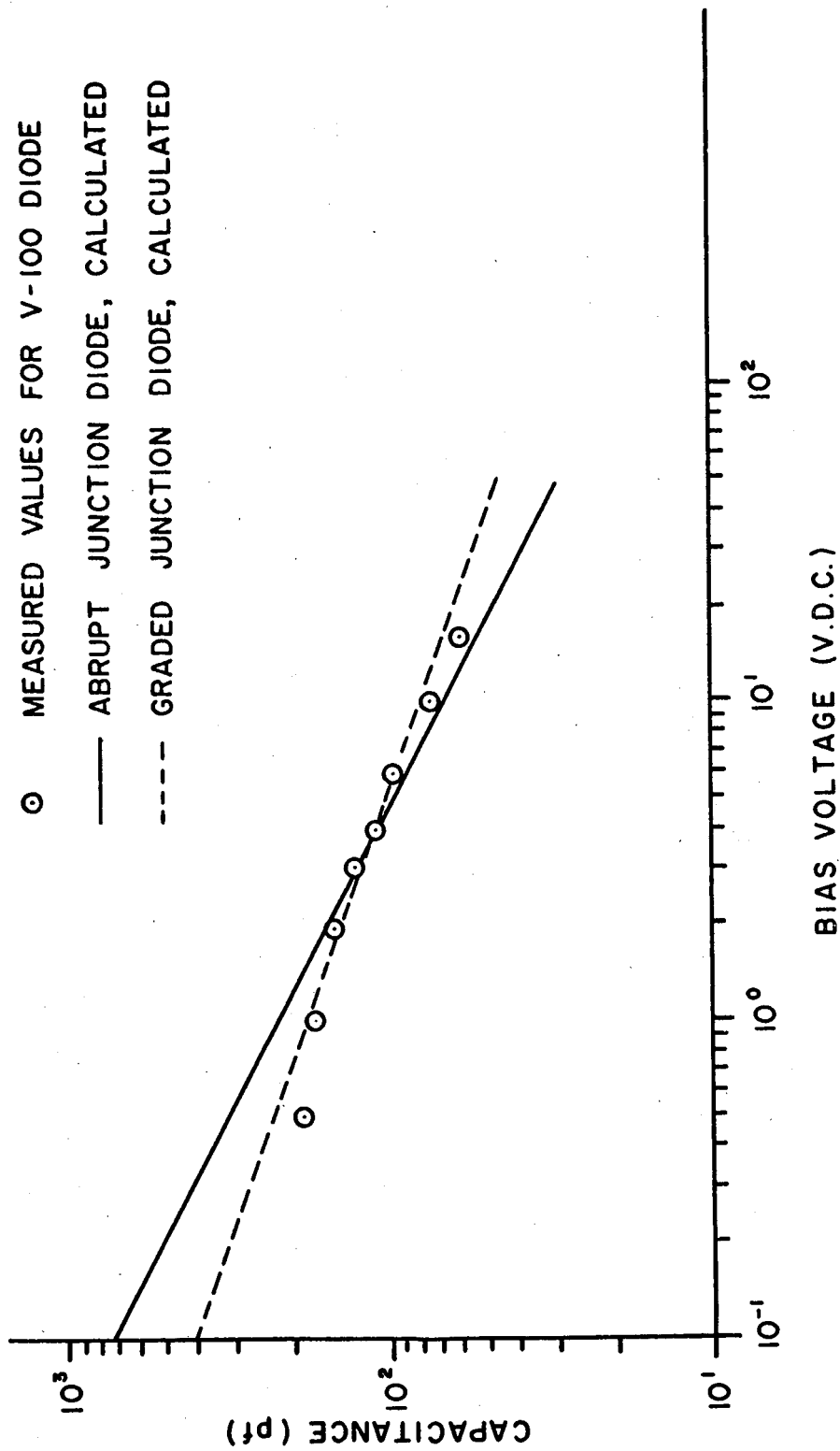
$V_c$  is the reverse-bias voltage and

$V_b$  is the junction contact potential.

The exponent n depends upon the geometry of the diode junction.

Giacoletto (1956) et al., have shown that the linearly graded junction has a capacitance which varies inversely with the cube root of the applied bias. The variation of capacitance with voltage for an abrupt junction follows an inverse square root relationship.

Type V-100 silicon diodes produced by Pacific Semiconductor, Inc., selected to be used in the bridge attenuator network, are of the abrupt junction type. Laboratory tests reveal, however, that these diodes do not exactly follow the inverse square root relationship.



CAPACITANCE VS. BIAS VOLTAGE

FIGURE 22

A graph of diode capacitance versus bias voltage for a typical V-100 diode is shown in Figure 22.

Also shown is the capacitance variation for the inverse square root and inverse cube root relationship of a PN diode.

The exponent  $n$  of the voltage sensitive capacitor was found to be 0.442 and the proportionality constant  $K$ , was  $205 \times 10^{-12}$  farads(volt)<sup>.442</sup>. It can also be seen from this graph that the capacitance sensitivity decreases at lower voltages because of the internal contact potential.

The variation of capacity  $C_{\max}$  to  $C_{\min}$  was found to be 3.5 for a 16 volt change of bias.

## A2 POWER LOSSES IN THE CAPACITY DIODE

The internal series resistance due to the semiconductor material of the PN junction is the major loss factor of the diode.

Since the series resistance and capacitance are frequency invariant, a figure of merit  $Q$ , may be defined as

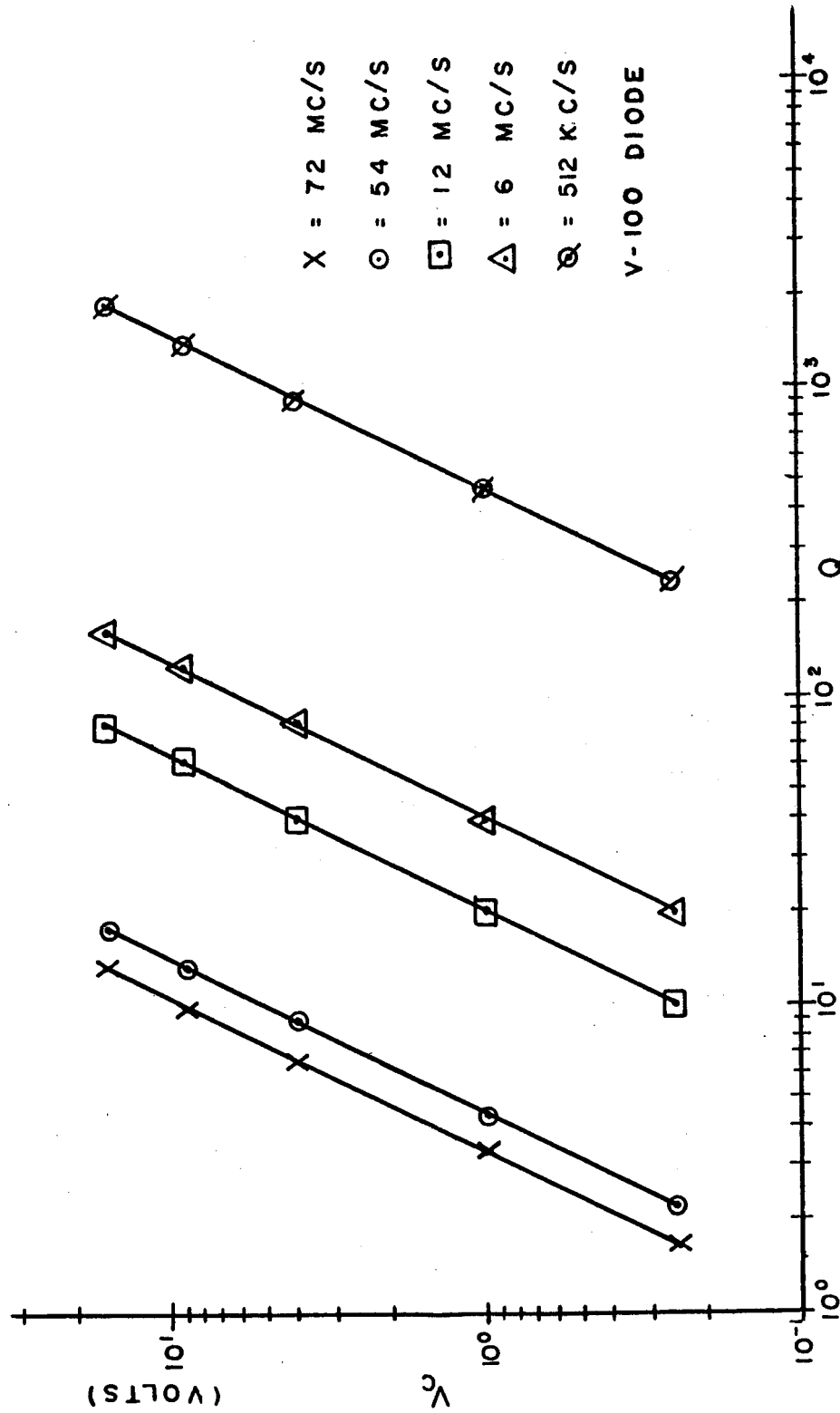
$$Q = 1 / \omega CR, \quad (A-1)$$

where  $C$  = voltage variable capacitance

$\omega$  = radian frequency and

$R$  = internal series resistance.

At 50 mc/s,  $Q = 11$ .



BIAS VOLTAGE VS FIGURE OF MERIT

FIGURE 23

Figure 23 shows the variation of Q with bias voltage for frequencies of 512 kc/s, 6mc/s, 12mc/s, 54mc/s, and 72mc/s.

Using equation 1, the equivalent series resistance is given by:

$$R = 1 / \omega C Q \quad (A-2)$$

for  $C = 73.5 \text{ pf.}$

$Q = 11$ , and

$$\omega = 3.39 \times 10^8 \text{ rad/ sec.}$$

$$R = 4 \text{ ohms} \quad (A-3)$$

### A3 THERMAL PROPERTIES

The thermal sensitivity of the capacity diode is attributed to its internal contact potential,  $V_b$ . To see how temperature affects the diode, consider the following equation<sup>15</sup> for a PN junction:

$$V_b = \frac{KT}{q} \ln \frac{AD}{n_i^2}, \quad (A-4)$$

where  $V_b$  = contact potential

$K$  = Boltzman's constant

$T$  = Absolute temperature, °K.

$q$  = electron charge

$A$  = Acceptor impurity concentration

$D$  = Donor impurity concentration

$n_i$  = intrinsic concentration.



Determination of contact voltage variation with temperature can be found using equation 4. The only unknown in this equation is the product AD; to deduce this product,  $V_b$  must be known at some temperature.

The first step, then, is to find the contact potential,  $V_b$ , at  $26^\circ \text{C}$ . It can be seen from Figure 22 that the capacitance follows the relationship

$$C = K / (V_c + V_b)^n \quad (\text{A-5})$$

where  $K$  = proportionality constant

$V_c$  = reverse-bias voltage

$V_b$  = contact potential

$n$  = the slope of the Capacitance vs. Voltage curve.

From equation 5,

$$V_b = (K/C)^{\frac{1}{n}} - V_c \quad (\text{A-6})$$

The following numerical values are from Figure 22 :

$$K = 205 \times 10^{-12} \text{ farads (volt)}^{0.442}$$

$$C = 188 \times 10^{-12} \text{ farads at } V_c = 0.5 \text{ volts}$$

$$V_c = 0.5 \text{ volts}$$

$$n = 0.442$$

Calculating  $V_b$  using equation 6,

$$V_b = 0.715 \text{ volts at } 26^\circ \text{C}. \quad (\text{A-7})$$

The product AD is not temperature dependent and can be found using equation 4, which is rearranged to yield,

$$\ln AD = \frac{V_b q}{kT} + \ln n_i^2 \quad . \quad (A-8)$$

Substituting the following values,

$$V_b = 0.715 \text{ volts at } 26^\circ\text{C}.$$

$$k = 1.38 \times 10^{-23} \text{ joule/}^\circ\text{K, Boltzman's constant}$$

$$q = 1.6 \times 10^{-19} \text{ coulombs}$$

$$T = 300^\circ\text{K}$$

$$\text{and } n_i^2 = 1.5 \times 10^{33} T^3 \exp -14,000/T, \text{ for Silicor(15).}$$

Equation 8 becomes,

$$\ln AD = 74.6 \quad (A-9)$$

At any temperature, equation 4 becomes,

$$V_b = \frac{kT}{q} [14,000/T - 3 \ln T - 1.9] \quad (A-10)$$

The internal contact potential varies from 0.715 volts at  $26^\circ\text{C}$ . to 0.62 volts at  $80^\circ\text{C}$ . and to 0.849 volts at  $-40^\circ\text{C}$ . This results in an approximately linear temperature sensitivity of about  $0.1\%/^\circ\text{C}$ . at 0.5 volts bias, about  $0.038\%/^\circ\text{C}$ . at 4 volts bias and becoming negligible at higher voltages.

## APPENDIX B

### DESCRIPTION OF THE 54MC/S PHASE COMPARATOR

The phase comparator used for the measurements described was designed by Space Craft Inc., Huntsville, Alabama.

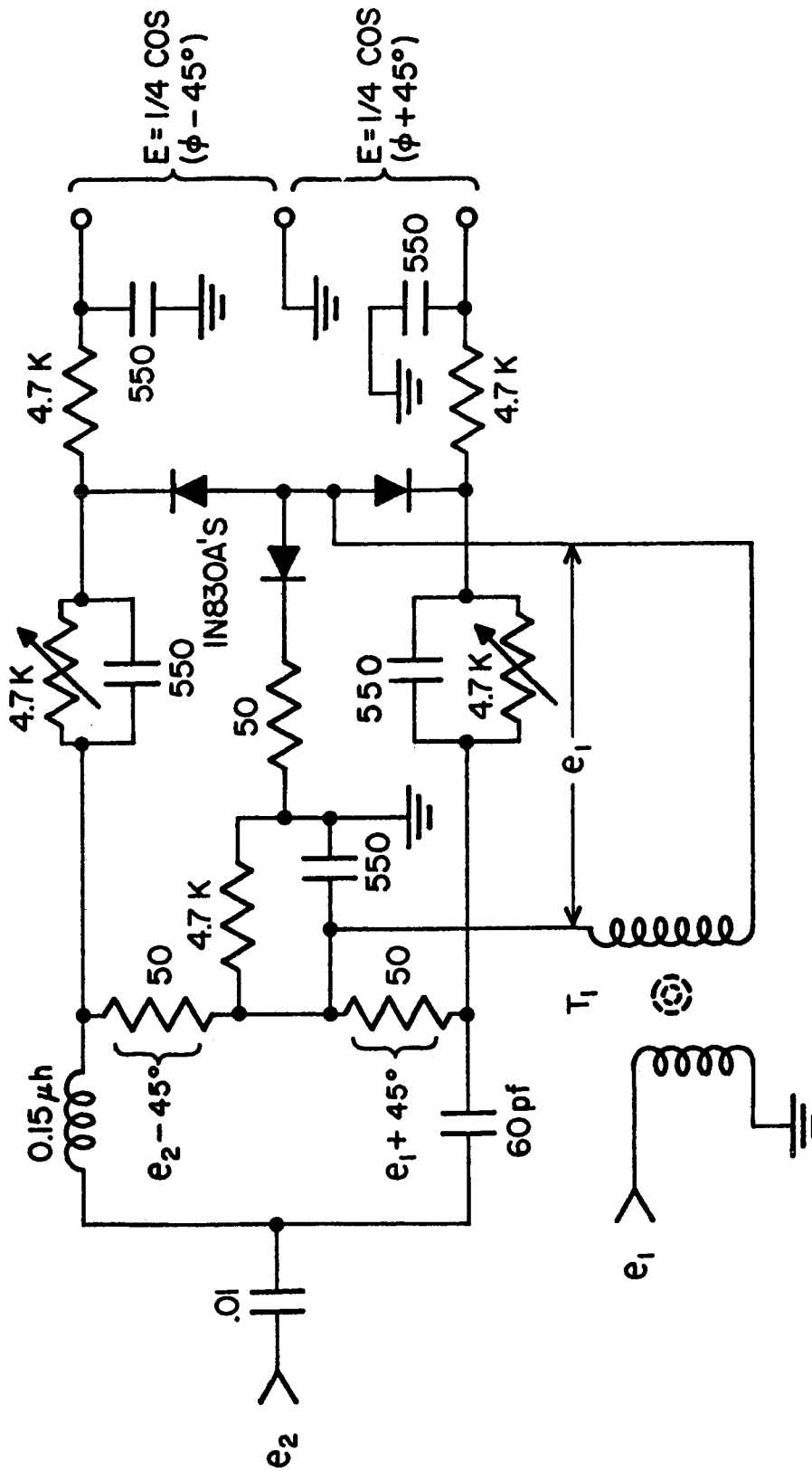
A schematic diagram of the phase comparator is shown in Figure 24 and its equivalent circuit in Figure 25. It may be noted in Figure 25 that  $e_1$  and  $e_2$  are to be compared in phase and  $e_1 \gg e_2$ . The resultant sum of the voltage approximately equals  $e_1 + e_2 \cos \theta$ ; the contact potentials of the diodes cancel. An additional diode is used to provide the quadrature output.

Two adjustable resistors are used to balance the back resistance of the diodes, resulting in an average output voltage of zero volts.

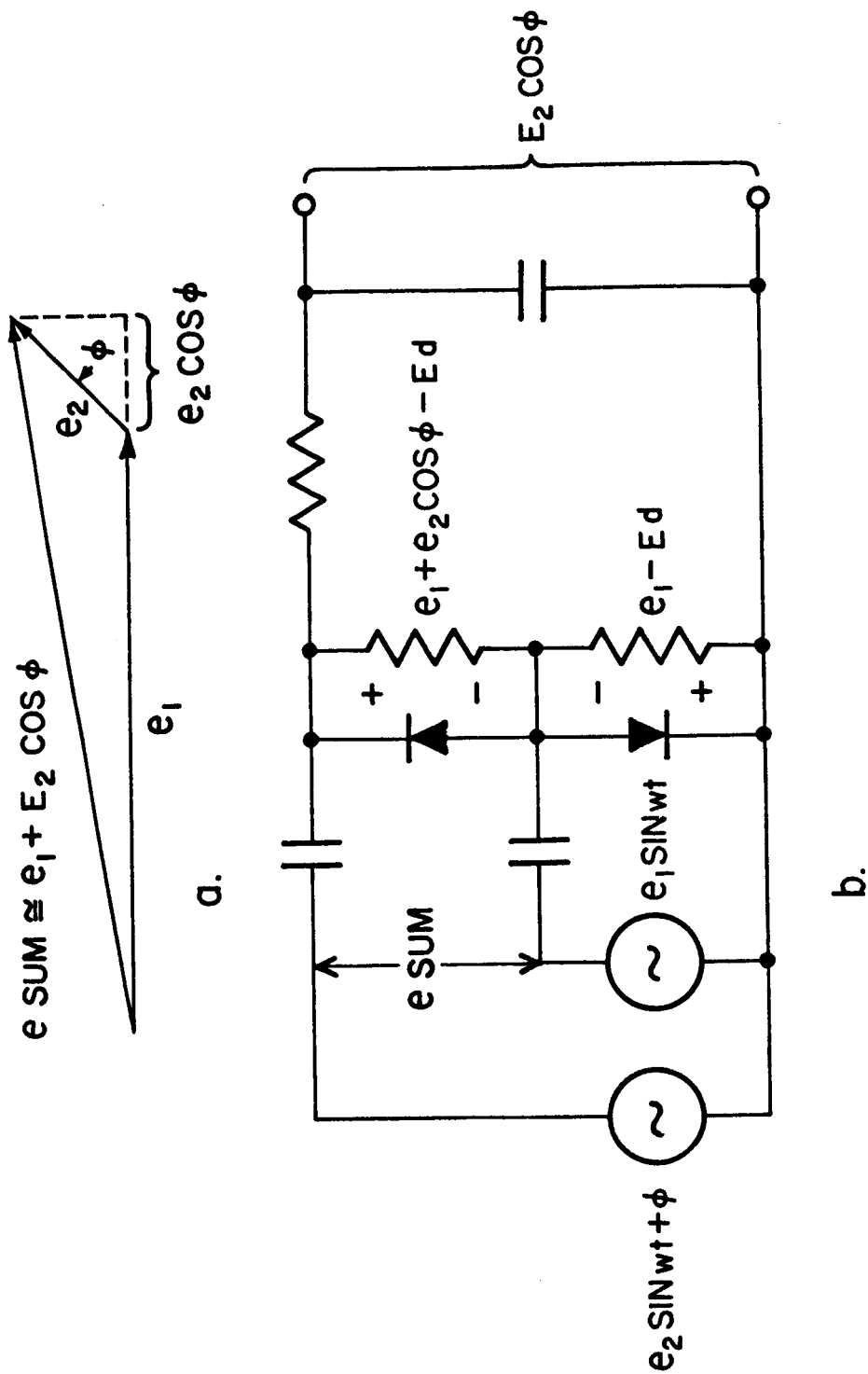
The  $\pm 45$  degree phase splitter for  $e_2$  is arranged so that the input is 50 ohms resistive.

Transformer  $T_1$ , is a high Q toroid with a voltage step-up ratio so as to make  $e_1 \gg e_2$ .

The d.c. output voltages of this comparator may be displayed on an oscilloscope to provide a polar plot of the phase angle between  $e_1$  and  $e_2$ .



PHASE COMPARATOR CIRCUIT  
FIGURE 24



PHASE COMPARATOR EQUIVALENT CIRCUIT

FIGURE 25

BIBLIOGRAPHY

1. Blecher, F.H., Automatic Gain Control of Junction Transistor Amplifiers, Proc. NEC., Vol. 9, 731, National Electronics Inc., Chicago, Ill., 1953.
2. Chow, W.F. and A.P. Stern, Automatic Gain Control of Transistor Amplifiers, Proc. IRE, 1119-1127, September 1955.
3. Chow, W.F. and H. Lazar, A New Method of Automatic Gain Control for HF and VHF Transistor Amplifiers, Solid-State Circuits Conference Digest of Technical Papers, 40-41, February 1959.
4. Fisher, Alan, Unpublished communication, Space Craft Inc., Huntsville, Ala., October 1962.
5. Fitchen, F.C., Transistor Circuit Analysis and Design, D. Van Nostrand Company, 1960.
6. Giacoletto, L.J. and J. O'Connell, A Variable Capacitance Germanium Junction Diode for UHF, RCA Review, 68, March 1962.
7. Hurtig, C.R., Constant Resistance Attenuator for Transistor Amplifiers, IRE Transactions on Circuit Theory, CT-2, 191-195, June 1955.
8. Kotzebue, K.L. and L.A. Blackwill, Semiconductor-Diode Parametric Amplifiers, Prentice-Hall, Inc., New Jersey, 1961.

9. Linvill, J.G. and J.F. Gibbons, Transistors and Active Circuits, McGraw-Hill Book Co., Inc., New York, 1961
10. Manley, J.M. and H.E. Rowe, Some General Properties of Non-Linear Elements, Proc. IRE. 44, 904-913, July 1956
11. McMahon, M.E. and L.S. Chase, Voltage Variable Capacitors -- State of the Art, Electronic Industries, 90-94, December 1959
12. McMahon, M.E. and G.F. Straube, Voltage Sensitive Semi-Conductor Capacitors, IRE Wescon Convention Records, Part 3, 72, August 1958
13. Nisbet, J.S. et al., Proposal for " A Study of Electron Densities in the Upper Atmosphere," Ionosphere Research Laboratory, The Pennsylvania State University, Scientific Report, No. 127, January 1960.
14. Phillips, A.B., Transistor Engineering, McGraw-Hill Book Co., Inc., New York, 1962.
15. Rossoff, A.L. and D. Dewitt, Transistor Electronics, McGraw-Hill Book Co., Inc., New York, 1957.
16. Seliga, T.A., " Phase Distortion in High Frequency Transistor Amplifiers," Ionosphere Research Laboratory, The Pennsylvania State University, Scientific Report, No. 153, December 1961.

17. Uhler, A., The Potential of Semiconductor Diodes in HF Communications, Proc. IRE., 46, 1099-1115, June 1958.
18. Wolfendale, E., The Junction Transistor and its Applications, The MacMillan Co., New York, 1958.
19. Selected Semiconductor Circuits, Prepared by Transistor Applications Inc., For Bureau of Ships, Department of the Navy, September 1959.